UNCLASSIFIED

AD 408 796

DEFENSE DOCUMENTATION CENTER

FOR

SCIENTIFIC AND TECHNICAL INFORMATION

CAMERON STATION, ALEXANDRIA, VIRGINIA

UNCLASSIFIED

NOTICE: When government or other drawings, specifications or other data are used for any purpose other than in connection with a definitely related government procurement operation, the U. S. Government thereby incurs no responsibility, nor any obligation whatsoever; and the fact that the Government may have formulated, furnished, or in any way supplied the said drawings, specifications, or other data is not to be regarded by implication or otherwise as in any manner licensing the holder or any other person or corporation, or conveying any rights or permission to manufacture, use or sell any patented invention that may in any way be related thereto.

RADC-TR-61-327

FINAL REPORT

Covering the Period
November 27, 1959
to
December 1, 1960

Research Program on Low-Noise Microwave Receiver Amplifying Devices

Prepared by:

A. Presser
F. Sterzer
G. Hodawanec and
H. Wolkstein

Approved by:

F. Vaccaro
M. Nowogrodzki

For

Radio Corporation of America
Missile Electronics and Control Division
Burlington, Massachusetts

by

Radio Corporation of America
Electron Tube Division
Microwave Tube Operations
Harrison, N. J.

Prime Contract AF30(602)-2115
P. O. No. GX 806067-L61

FOREWORD

This report gives the results of a research and evaluation study on low-noise microwave receiver amplifier devices. The study program was carried out in two parts. Part 1 consisted of a research into the feasibility of using tunnel-diode and parametric devices as low-noise L-band amplifiers. Part 2 dealt with the development of a very low noise, S-band traveling-wave amplifier.

The program was initiated by the Missile Electronics and Control Division of the Radio Corporation of America, under prime Air Force Contract AF30(602)-2115 (on purchase order No. GX 806067-L61). The work was carried out by the Electron Tube Division of the Radio Corporation of America — Part 1 by the Microwave Advanced Development Group at Princeton, N. J., and Part 2 by the Microwave Design and Development Group at Harrison, N. J.

TABLE OF CONTENTS

TABLE OF CONTENTS (CONT.)

LIST OF ILLUSTRATIONS

LIST OF ILLUSTRATIONS (CONT.)

LIST OF ILLUSTRATIONS (CONT.)

ABSTRACT

PART 1

RESEARCH STUDIES ON LOW-NOISE TUNNEL DIODES AND PARAMETRIC DEVICES

Two low-noise, L-band tunnel-diode amplifiers were built and delivered. Both amplifiers had voltage-gain-bandwidth products exceeding the objective specifications. The amplifiers fitted inside a metal box of dimensions 7" x 3-1/2" x 0.4", and required about 2 mw of dc power (0.2 volt at 10 ma). The best experimental results were as follows: Center frequency = 1270 mc, Bandwidth = 64 mc, Gain = 26 db, Noise figure ≈ 5 db.

Three parametric subharmonic oscillators (pump frequency = 5700 mc, signal frequency = 2850 mc) were built and delivered. The size of the oscillators (excluding connectors) was 3-1/2" x 1.3" x 1/8". All oscillators met the objective specifications.

A four-terminal low-noise modulate-demodulate L-band parametric amplifier was built and tested. The best experimental results were as follows: Center frequency = 1200 mc, Bandwidth = 2.2 mc, Gain = 29 db, Noise figure ≈ 2.5 db.

PART 2

DEVELOPMENT OF A VERY LOW NOISE, S-BAND TRAVELING-WAVE TUBE

This part of the report describes the development of a traveling-wave-tube amplifier which has demonstrated a capability for very low noise operation in the S-band range of microwave frequencies.

Much of the effort expended on this program was of an exploratory nature, aimed at determining the feasibility of achieving very low noise operation in a simplified and practical traveling-wave tube design. This effort included theoretical studies concerning noise reduction in beam devices, coupled with experimental tests. The theoretical design approaches are discussed separately in the Scientific Reports issued as part of this program.

The practical design approaches followed ~~on this program~~ consider such factors in low-noise traveling-wave-tube design as the cathode, the beam-impedance transformation, and the rf sections. ~~Critical factors in these areas~~ are ~~discussed with regard to low-noise performance.~~ Emphasis is placed upon the electron gun design, favorable launching conditions for hollow electron beams, and the magnetic field configuration required for optimum low-noise performance. ~~In addition,~~ a beam-focusing technique is described which ~~not only~~ permits a considerable reduction in size, weight, and power dissipation of the focusing

solenoid, but also enables a much improved small-signal gain and saturated power output characteristic, with no adverse effect on the low-noise performance of the tube.

The final tube design, ~~which can be used for front-end receiver operation, has~~ achieved minimum tube noise figures as low as 2.6 db and broadband noise figures of less than 3.5 db in the 2100 - 3500 mc frequency range. Broadband tube noise figures were nominally in the order of 3 - 4 db, with small-signal gains in the order of 30 db and saturated power outputs in the order of 2 - 3 mw.

PART 1

RESEARCH STUDIES ON LOW-NOISE TUNNEL DIODES AND PARAMETRIC DEVICES

PART 1

RESEARCH STUDIES ON LOW-NOISE TUNNEL DIODES AND PARAMETRIC DEVICES

I. INTRODUCTION

In this part of the program, a feasibility study was conducted to determine if three solid-state devices could be successfully developed for use in a low-noise microwave receiver. The devices studied were:

1. A low-noise, L-band tunnel-diode amplifier
2. An S-band, subharmonic parametric oscillator
3. A four-terminal, low-noise, L-band parametric amplifier

Theoretical and empirical analyses were made to determine optimum circuit parameters and to predict performance characteristics of these devices. Practical devices of each type were built and evaluated.

In the following paragraphs, the objective specifications for each device are given, and the results of the activities carried out to achieve these objectives are reported.

II. OBJECTIVES

The specific activities to be carried out in this part of the program were:

1. To develop a low-noise tunnel-diode amplifier to meet the following specifications:

Frequency	L-band
Bandwidth	5 per cent
Gain	10 db
Noise figure	5 db

Two such amplifiers, meeting the objective specifications, were to be delivered at the conclusion of the project. The amplifier design was required to be sufficiently flexible to permit the development of a scaled version to operate at S-band frequencies.

2. To build and deliver three subharmonic parametric oscillators with a pump frequency of 5700 mc and a signal frequency of 2850 mc.

3. To build and test a four-terminal, low-noise, modulate-demodulate, L-band parametric amplifier.

III. LOW-NOISE, L-BAND TUNNEL-DIODE AMPLIFIER

Tunnel diodes are heavily doped p-n junctions that exhibit an incremental negative resistance at small forward dc bias. These diodes hold great promise for high-frequency applications because they are not limited by transit-time effects, even at microwave frequencies.

This section is concerned with the use of tunnel diodes in low-noise microwave amplifiers. First, the diode parameters that determine the performance of the diode in amplifier circuits are described in some detail. Next, expressions for gain, bandwidth and noise figure are derived. Finally, a practical amplifier circuit is described and experimental results are given.

A. Tunnel-Diode Parameters

An approximate equivalent circuit for an encapsulated tunnel diode consists of three elements connected in series: an inductance L_d, a resistance r_d, and a voltage-dependent resistance R_d shunted by a voltage-dependent capacitance C_d, as shown in Fig. 1. L_d results mainly from the inductance of the housing; r_d is the resistance of the ohmic contact, the base, and the internal leads of the

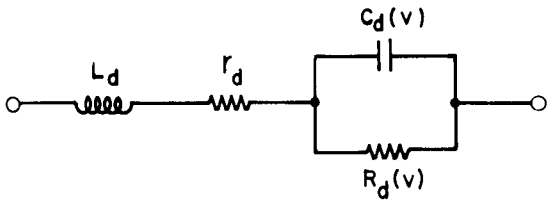

Fig. 1 — Equivalent circuit of tunnel diode

package. $C_d(v)$ is the junction capacitance, and $[R_d(v)]_o$ is the resistance of the junction.

The dc bias voltage V_d across a tunnel diode is given by

$$V_d = I_d r_d + I_d [R_d(v)]_o \tag{1}$$

where I_d is the direct current through the diode. At a reverse current an order of magnitude greater than I_p, $[R_d]_o$ is usually very small compared to r_d, so that r_d can be measured directly. When r_d is known, $[R_d]_o$ can be determined from the current-voltage characteristics of the diode.

Figure 2 shows the current-voltage characteristics of a typical germanium tunnel diode. Presently available microwave diodes have values of I_p varying from about one quarter ma to a few hundred ma. The ratio of I_p to I_v (I_v is the value of current corresponding to V_v) usually exceeds 5:1. Ratios of better than 20:1 have been obtained.

In ac applications, the quantity of most interest is not the absolute value of the junction resistance, $[R_d(v)]_o$, but rather its incremental value $R_d(v)$. Fig. 2 indicates that for a typical germanium tunnel diode R_d is negative over a voltage range from 0.065 volt to 0.28 volt.

The series inductance L_d and the junction capacitance $C_d(v)$ of a tunnel diode can be determined from ac impedance measurements. Theoretically, the variation of C_d with voltage, when V_d is less than V_v, may be approximated by

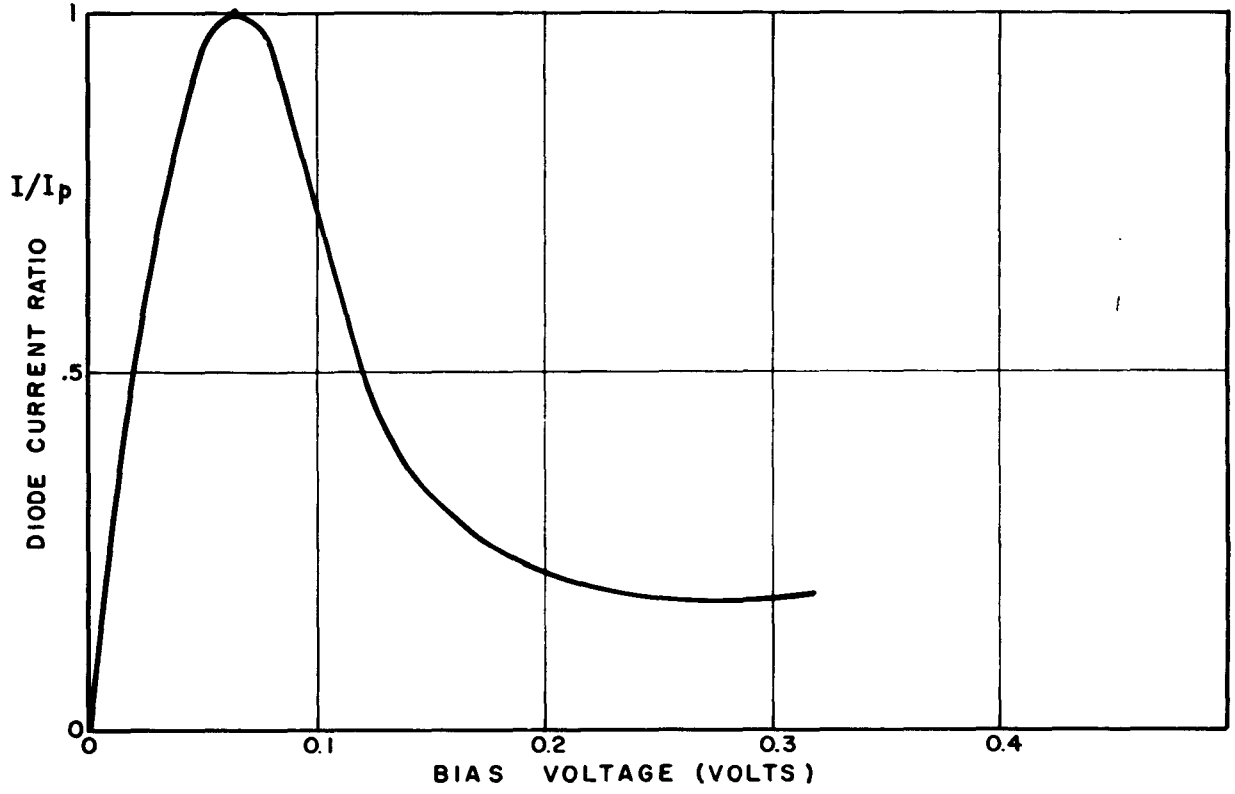

Fig. 2 — Current-voltage characteristics of a typical germanium diode

$$C_d(v) = K(\phi - v)^{-1/2} \tag{2}$$

where K and ϕ are constants. Fair agreement between experimental values of C_d and the values predicted from Eq. (2) may be obtained by setting the value of ϕ equal to 0.6 volt for germanium

B. Impedance of Tunnel Diodes

In terms of the incremental resistance R_d, the impedance, Z_d, of a tunnel diode may be written as follows:

$$Z_d = \left(r_d - \frac{|R_d|}{R_d^2 C_d^2 \omega^2 + 1} \right) + j \left(\omega L_d - \frac{R_d^2 C_d \omega}{R_d^2 C_d^2 \omega^2 + 1} \right) \tag{3}$$

where it is assumed that the diode is biased in a region where R_d is negative.[1] In order that the diode exhibit negative resistance, R_d must be greater than r_d. The real part of the impedance, $Re(Z_d)$, is equal to $(r_d - R_d)$ at zero frequency and increases monotonically with frequency. The frequency at which $Re(Z_d)$ becomes zero is called the cutoff frequency f_c, and is given by

$$f_c = \frac{\sqrt{\frac{|R_d|}{r_d} - 1}}{2\pi |R_d| C_d} \tag{4}$$

---

1. Unless otherwise noted, it will be assumed throughout this report that R'_d is negative.

At frequencies above f_c, $Re(Z'_d)$ is positive, and the diode exhibits a passive impedance. The bias voltage corresponding to a maximum value of f_c is usually very close to the voltage corresponding to a minimum value of $|R_d|$.

The imaginary part of Z'_d, $Im(Z'_d)$, becomes zero at frequency f_r, where

$$f_r = \frac{\sqrt{R_d^2 \frac{C_d}{L_d} - 1}}{2\pi |R_d| C_d} \tag{5}$$

Usually f_r is referred to as the self-resonant frequency of the diode. Below self-resonance, the reactance of the diode is capacitive; above self-resonance, it is inductive.

C. Stability of Tunnel-Diode Circuits

The characteristic equation of a tunnel diode circuit can be found in the conventional manner by using the generalized frequency, $s = \sigma + j\omega$, in the expression for either the impedance or admittance of the circuit. In general, the characteristic operation will have an infinite number of eigen frequencies, $s_n = \sigma_n + j\omega_n$. If σ_n is greater than zero, then oscillations can occur at frequency ω_n. However, if there exists no σ_n greater than zero, the circuit will be stable.

In general it does not seem possible to stabilize a circuit containing a tunnel diode for which[2]

---

2. D. E. Nelson and F. Sterzer, "Tunnel Diode Microwave Oscillators with Milliwatt Power Output," 1960 WESCON Convention Record.

$$L_d > |R_d|^2 C_d \tag{6}$$

Tunnel diodes are useful as conventional amplifiers only at frequencies below their cutoff frequency, f_c. From Eq. (5), it can be seen that high values of f_c result from small values of R_d, C_d, and r_d. However, the smaller the values of R_d and C_d, the smaller the inductance L_d of the diode must be to satisfy inequality of Eq. (6). In our amplifiers, we are using tunnel diodes packaged in low inductance RCA mounts. The inductance of those special diodes is only 350 $\mu\mu$h.

D. Calculation of Gain and Bandwidth of Tunnel Diode Amplifiers

Tunnel diodes are two-terminal devices. A useful amplifier, however, must in general be a three-terminal device, i.e., the amplifier must have separate input and output terminals. At microwave frequencies, the most convenient method of obtaining a three-terminal tunnel diode amplifier is to use a ferrite circulator.

Figure 3 shows a tunnel diode amplifier using a three-port circulator. Ports 1 and 3 of the circulator serve as input and output ports, respectively. Port 2 is connected to the tunnel diode circuit.

Assuming an ideal circulator, the power gain G_p of the amplifier can be written in terms of the voltage reflection coefficient Γ_v of the tunnel diode circuit

$$G_p = |\Gamma_v|^2 = \frac{(G_0 - G_c)^2 + B_c^2}{(G_0 + G_c)^2 + B_c^2} \tag{7}$$

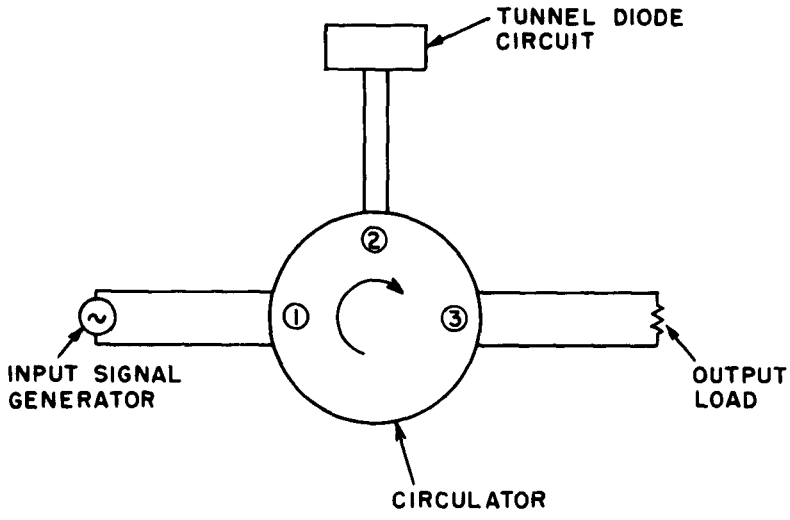

Fig. 3 — Schematic of tunnel-diode amplifier

where

G_0 = characteristic admittance of transmission line feeding the tunnel diode circuit (see Fig. 3)

$Y_c = G_c + jB_c$ = admittance of the tunnel diode circuit at junction of the circuit and the transmission line.

Equation (7) shows that G_p will be bigger than one, if, and only if, G_c is less than zero.

Both gain and bandwidth of a tunnel diode amplifier can be calculated from Eq. (7). In general, however, the frequency dependence of Y_c is quite complicated, and Eq. (7) must be solved graphically to determine the bandwidth.[3]

E. Calculation of Noise Figure of Tunnel-Diode Amplifiers

The noise figure of a tunnel-diode amplifier at resonance (i. e. at the frequency where $B_c = 0$) can be written as[4]

$$F = 1 + \frac{4T}{T_0} \frac{G_g G_e \left[\frac{G_1}{G_e} + \frac{r_d}{R' - r_d} + \frac{e I_0 |R_d| R'}{2KT(R' - r_d)} \right]}{(G_g - G_1 - G_e)^2} \tag{8}$$

---

3. In low-frequency applications it is often possible to neglect the effect of the series inductance and resistance of the diode. In this case, the voltage-gain-bandwidth product of single tuned amplifiers is given by $1/\pi R_d C_d$.

4. See, for example, M. E. Hines and W. W. Anderson, "Noise Performance Theory of Esaki (Tunnel) Diode Amplifiers," Proc. IRE, April 1960.

where

T = circuit temperature

T_o = reference temperature

I_o = dc diode current

k = Boltzman's constant

e = charge of the electron

G_g = generator conductance = G_o

G_l = circuit loss conductance

$$R' = \frac{|R_d|}{1 + (\omega C_d R_d)^2} \; ; \; \omega = 2\pi f$$

f = resonance frequency

$$G_e = \frac{R' - r_d}{(r_d - R')^2 + \omega^2 (L_d - C_d |R_d| R')^2}$$

For high gain, ($G_c \rightarrow G_o$) Eq. (8) becomes

$$F = 1 + \frac{T}{T_0} \left[\frac{G_e}{G_e - G_l} \right] \left[\frac{G_l}{G_e} + \frac{e I_0 |R_d|}{2kT} \right] \tag{9}$$

If $T = T_o$, and there is no loss ($G_l = 0$), Eq. (9) reduces to

$$F = 1 + \frac{e I_0 |R_d|}{2kT_0} = 1 + 20(I_0 |R_d|) \tag{10}$$

$$T_0 = 290^\circ K$$

For presently available tunnel diodes, $1 + 20\,(I_o|R_d|)_{min.}$ is in the vicinity of 3.5 db.

F. Experimental Results

A number of amplifiers operating in the frequency range from about 800-1500 mc were built. In general, fair agreement was obtained between measured and calculated results.

The best results were obtained with the amplifier shown schematically in Fig. 4. This amplifier was used with a special RCA germanium tunnel diode with the following characteristics:

$I_p = 4$ ma

$|R_d|_{min} \approx 25$

$L_d = 350\ \mu\mu h$

$C_d = 13\ \mu\mu f$

$r_d = 1.1$ ohms

Figure 5 is a plot of the conductance and susceptance of this diode versus frequency. It can be seen that below 1600 mc the diode conductance is almost frequency independent, and the diode susceptance varies almost linearly with frequency.

Figure 6 shows the power gain of the amplifier versus frequency. The maximum power gain is about 26 db (f = 1290 mc) and the bandwidth about 64 mc (voltage-gain-bandwidth product = 1280 mc). In Fig. 7, output power is plotted versus input power. It can be seen that the amplifier is linear for output powers up to about -30 dbm. The noise figure of this amplifier is about 5 db.

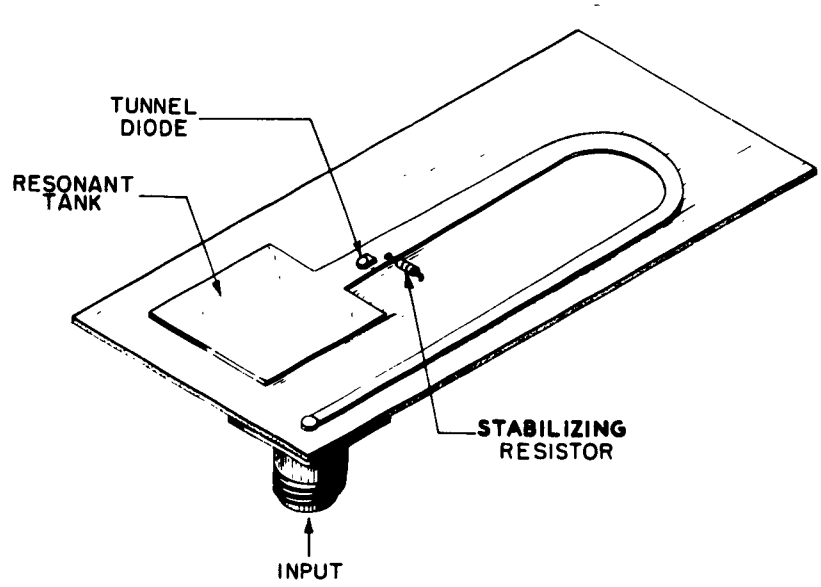

Fig. 4 — L-band tunnel-diode amplifier

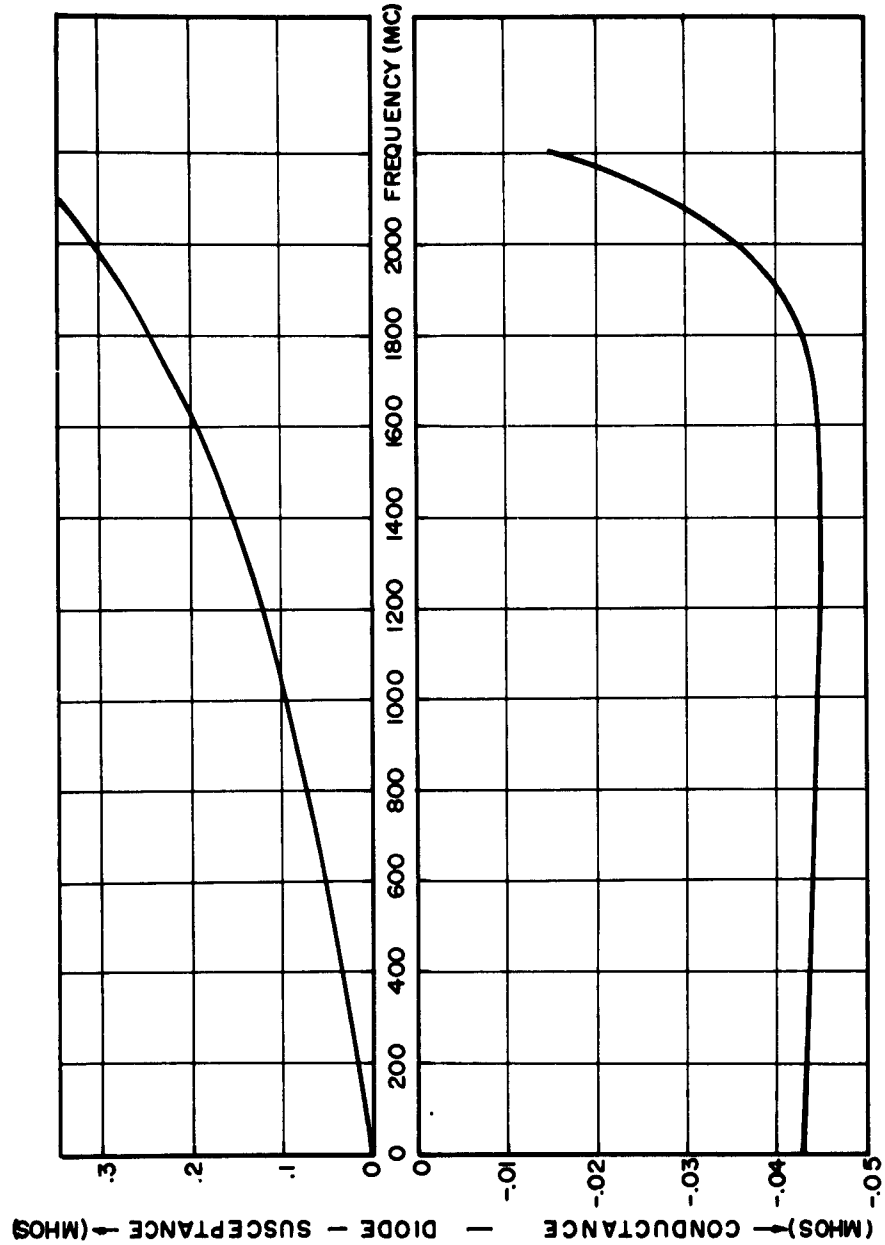

Fig. 5 — Admittance characteristics of the L-band tunnel-diode amplifier. (a) Susceptance versus frequency. (b) Conductance versus frequency.

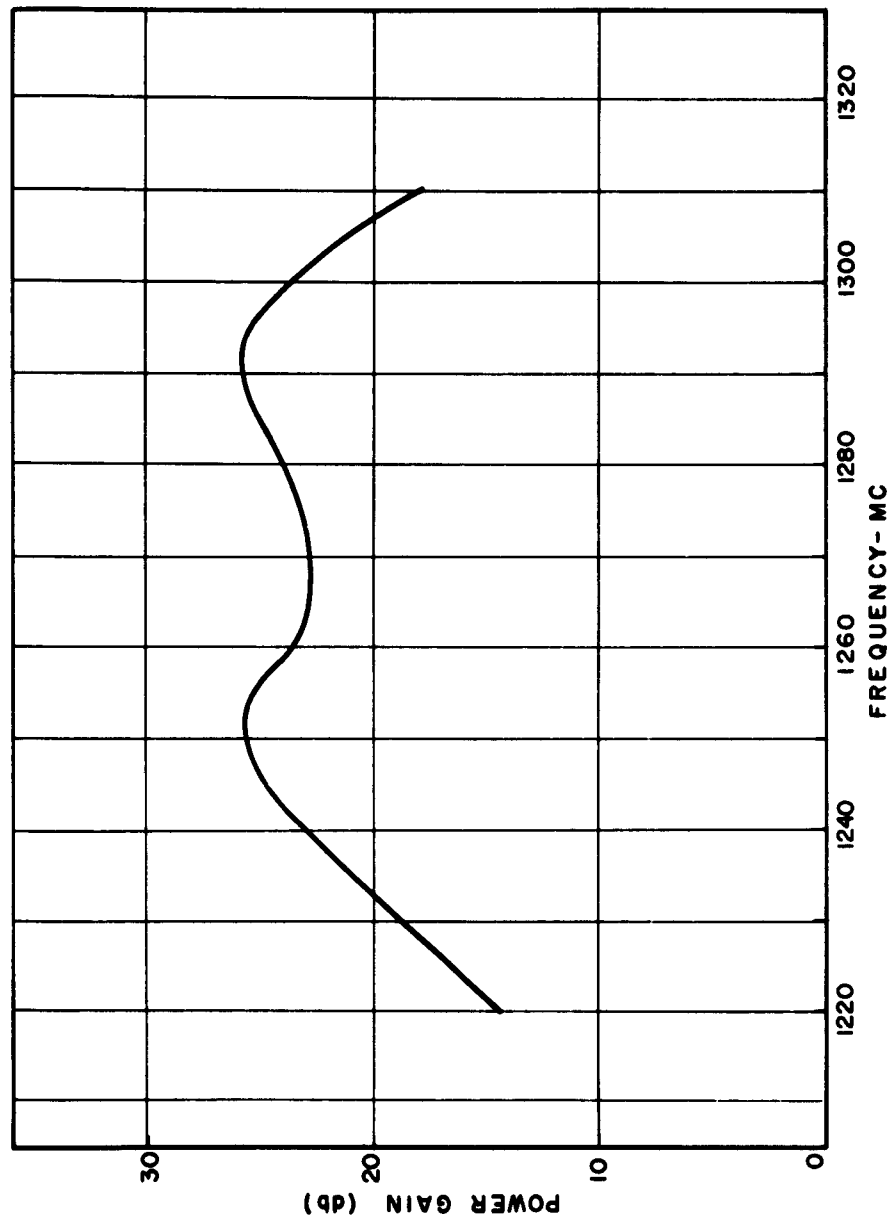

Fig. 6 — Power gain of the L-band tunnel-diode amplifier versus frequency

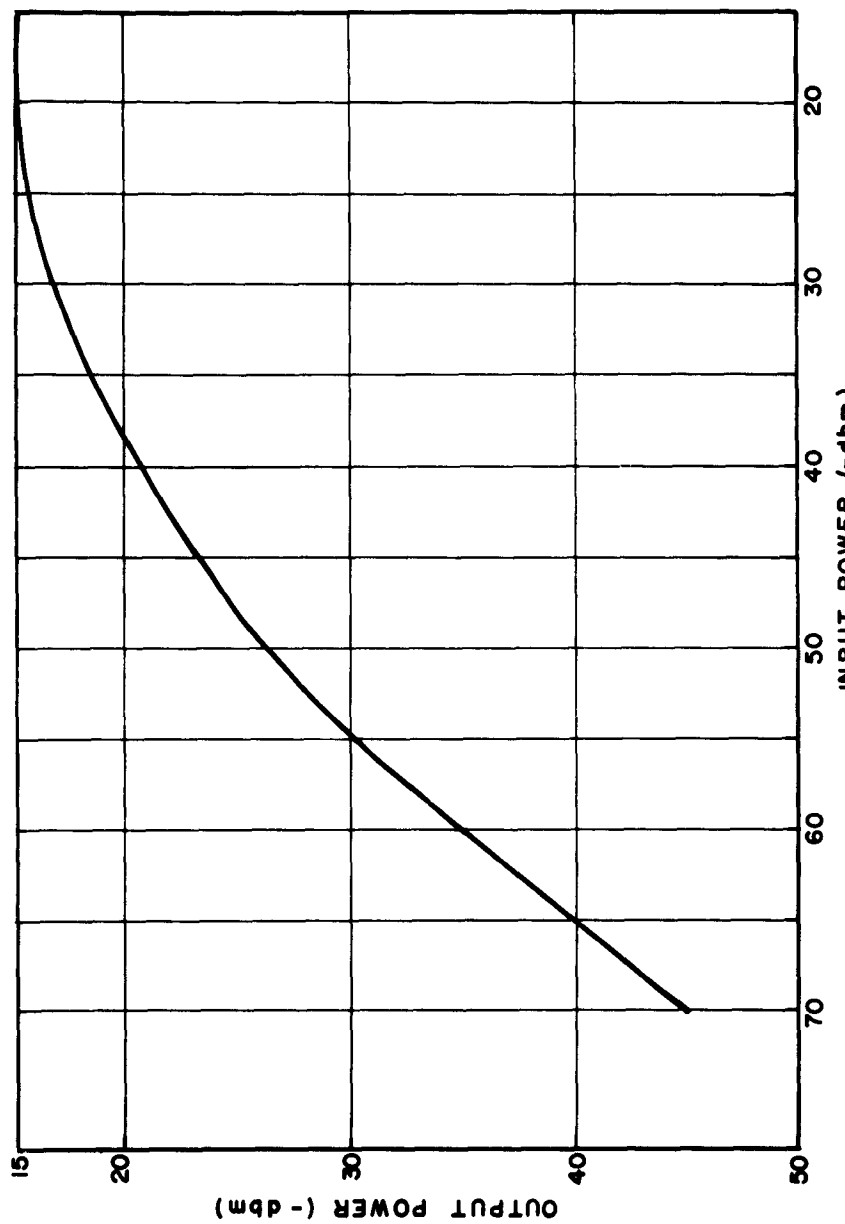

Fig. 7 — Output power of the L-band tunnel-diode amplifier versus input power

Two amplifiers of the type shown in Fig. 4 were delivered. Both amplifiers had gain-bandwidth products exceeding the objective specifications.

G. Scaling of L-Band Amplifier to S-Band

The amplifier shown in Fig. 4 can be readily scaled to S-band. For operation at 3000 mc, tunnel diodes with the following parameters must be used:

$R_{d\,(min)} = 140$ ohms

$C_d = 1.5\ \mu\mu f$

$L_d \approx 350\ \mu\mu h$

$r_d = 3$ ohms

Diodes of this type have been made on an experimental basis at the RCA Laboratories.

IV. S-BAND SUBHARMONIC PARAMETRIC OSCILLATORS

When a variable reactor is driven from a source, or pump, having a frequency f, a negative conductance is established across the reactor at or near the frequency f/2. (If the reactance is a nonlinear function of the drive, this negative conductance can also be developed at f/3, f/4 ,..., f/n). When connected to a low-loss circuit tuned to f/2, this negative conductance can overcome the circuit loss and produce stable oscillations at the frequency f/2 (i.e., subharmonic oscillations).[5]

---

5. The theory and application of parametric subharmonic oscillators is discussed in detail in the following two references: E. Gotto, "The Parametron, A Digital Computing Element which Utilizes Parametric Oscillations," Proc. IRE, Aug. 1959, and F. Sterzer, "Microwave Parametric Subharmonic Oscillators for Digital Computing," Proc. IRE, Aug. 1959.

Figure 8 shows a subharmonic oscillator, built from a shielded-strip transmission line, which produces an output of 2850 mc (pump frequency = 5700 mc). The important elements of this oscillator are: a 2850-mc half-wave resonator containing a variable-capacitance diode; a 5700-mc half-wave resonant bar (filter), which permits the 5700-mc pump power to enter the resonant tank, but prevents 2850-mc oscillation power from escaping; and two coaxial connectors (type N) for pump input and signal output. Both the resonant tank and the filter are shielded with copper foil to prevent any radiation losses.

Three oscillators of the type shown in Fig. 8 were built and delivered. These oscillators used special RCA variable-capacitance germanium junction diodes. The cutoff frequencies of these diodes ranged from 50 to 80 kmc. The diodes were encapsulated in a ceramic cylinder of 0.040 inch height and 0.085 inch outside diameter. The packaged diode fitted into a hole drilled into the strip transmission line.

The three subharmonic oscillators operated satisfactorily with pump powers in the range 15 to 30 mw.

V. FOUR-TERMINAL, LOW-NOISE PARAMETRIC L-BAND AMPLIFIER

A four-terminal, low-noise modulation-demodulation (M-D), L-band parametric amplifier was built and tested. This M-D amplifier combines the advantages of parametric up-converters and negative resistance amplifiers. With only a single parametric element, and without using a circulator, the amplifier has the following characteristics: input and output are at the same frequency,

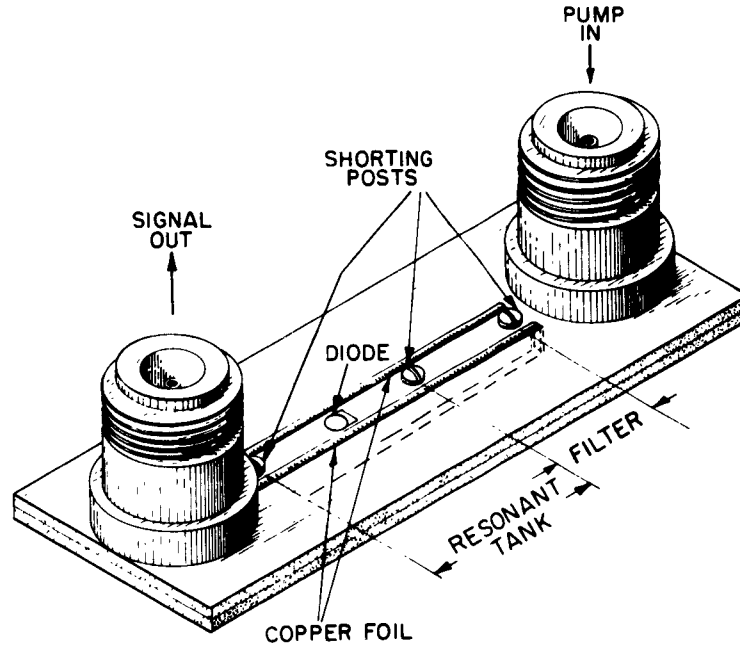

Fig. 8 — S-band subharmonic parametric oscillator

unidirectional gain is obtained between separate input and output ports, and the gain is relatively insensitive to variations in pump power and load impedance.

Figure 9 is a schematic block diagram of the basic amplifier, which consists of an amplitude modulator followed by a demodulator. Figure 10 shows a simplified equivalent circuit. In the non-linear capacitance modulator, an rf pump at frequency f_p is amplitude modulated by the input signal, f_s. Both upper $(f_p + f_s)$ and lower $(f_p - f_s)$ sidebands are produced. It is well known that if only the upper sideband is allowed to exist, as in the parametric upper-sideband up-converter, unconditionally stable gain can be obtained, but in this case the maximum attainable gain is limited to the ratio $(f_p + f_s)/f_s$. If only the lower sideband exists, on the other hand, as in the parametric lower-sideband up-converter, the gain is not limited by the ratio $(f_p - f_s)/f_s$, but negative resistance is produced at both $(f_p - f_s)$ and at f_s, and therefore, the gain is only conditionally stable. However, if there is power flow at both sideband frequencies, as in the modulator used in the M-D amplifier, then stable gain can be obtained which is not limited by any frequency ratio.

In order to have the output of the amplifier at frequency f_s, the modulated carrier is fed into a non-linear resistance amplitude demodulator. In this demodulator the power contained in both sidebands is converted to output power at frequency f_s. The demodulator has a conversion loss of several db. However, if the modulator has sufficient gain, the overall gain of the M-D amplifier can be very high.

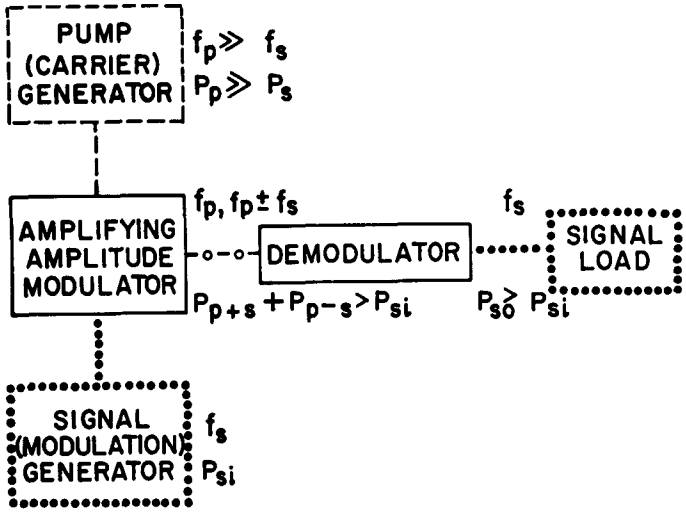

Fig. 9 — Block diagram of modulator-demodulator parametric amplifier

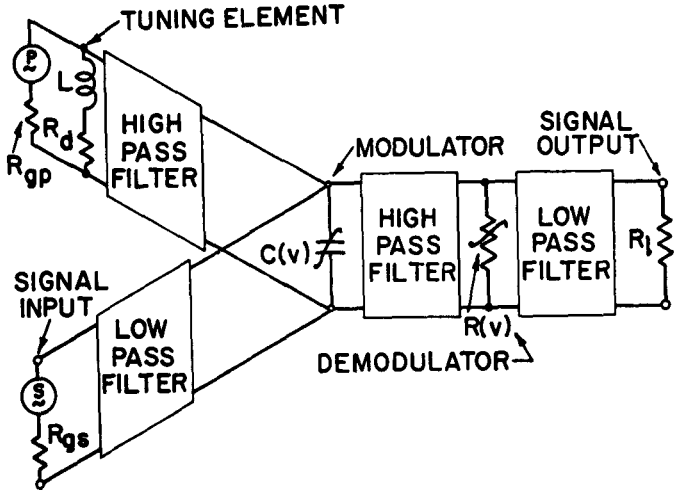

Fig. 10 — Simplified equivalent circuit diagram of a modulator-demodulator amplifier

Figure 11 is a photograph of the actual amplifier. The pump frequency is 10 kmc.

The performance of this amplifier, operating at a frequency of about 1.2 kmc is summarized in Figs. 12, 13 and 14. Fig. 12 shows the forward gain and reverse loss for two different adjustments of the tuning elements. The maximum voltage-gain-bandwidth product measured was about 70 mc. Fig. 13 is a plot of power gain versus pump power. It can be seen that the gain of the amplifier is relatively insensitive to pump power variations at high pump power levels. Figure 14 is a plot of input power versus output power, showing that the amplifier saturates with an input power of 0.1 mw.

The equivalent noise temperature of the variable-capacitance modulator is small compared to the noise temperature of the variable-resistance demodulator. Therefore, to minimize the noise figure of a M-D amplifier the gain in the modulator should be made very high, so that the noise contribution of the demodulator becomes negligible, as far as the overall amplifier noise figure is concerned. For a tuning adjustment which provides a gain of 30 db, the measured noise figure was about 2.5 db.

VI. CONCLUSIONS

1. Compact low-noise, L-band tunnel-diode amplifiers can be built in sizes that are compatible with use in phase-array antennas.

2. Four-terminal, low-noise L-band parametric amplifiers can be constructed using the modulate-demodulate principle.

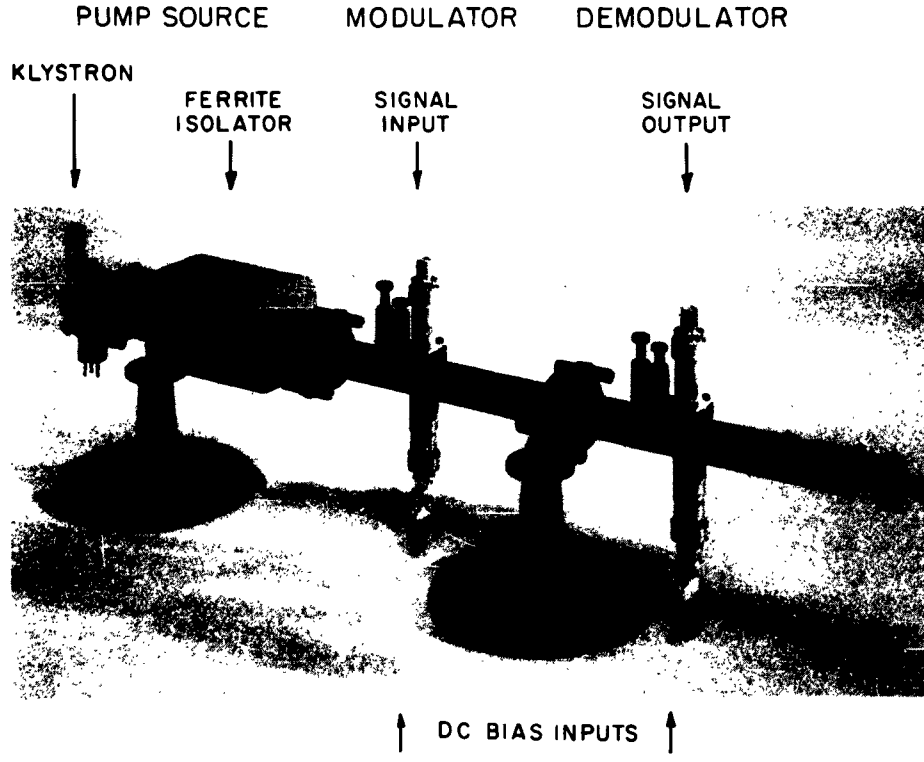

Fig. 11 — External view of the modulator-demodulator parametric amplifier

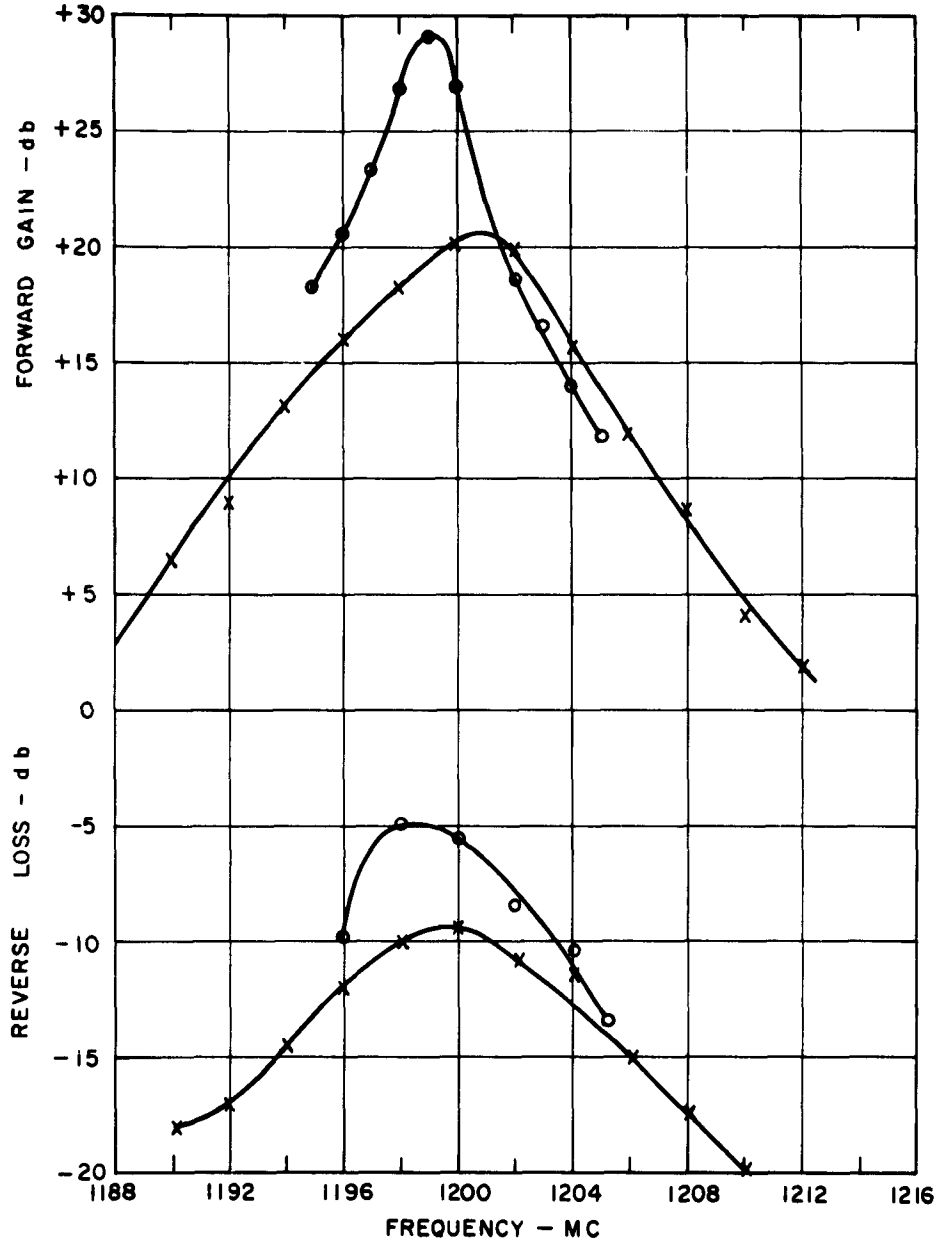

Fig. 12 — Forward gain and reverse loss versus frequency for two adjustments of the modulator-demodulator amplifier

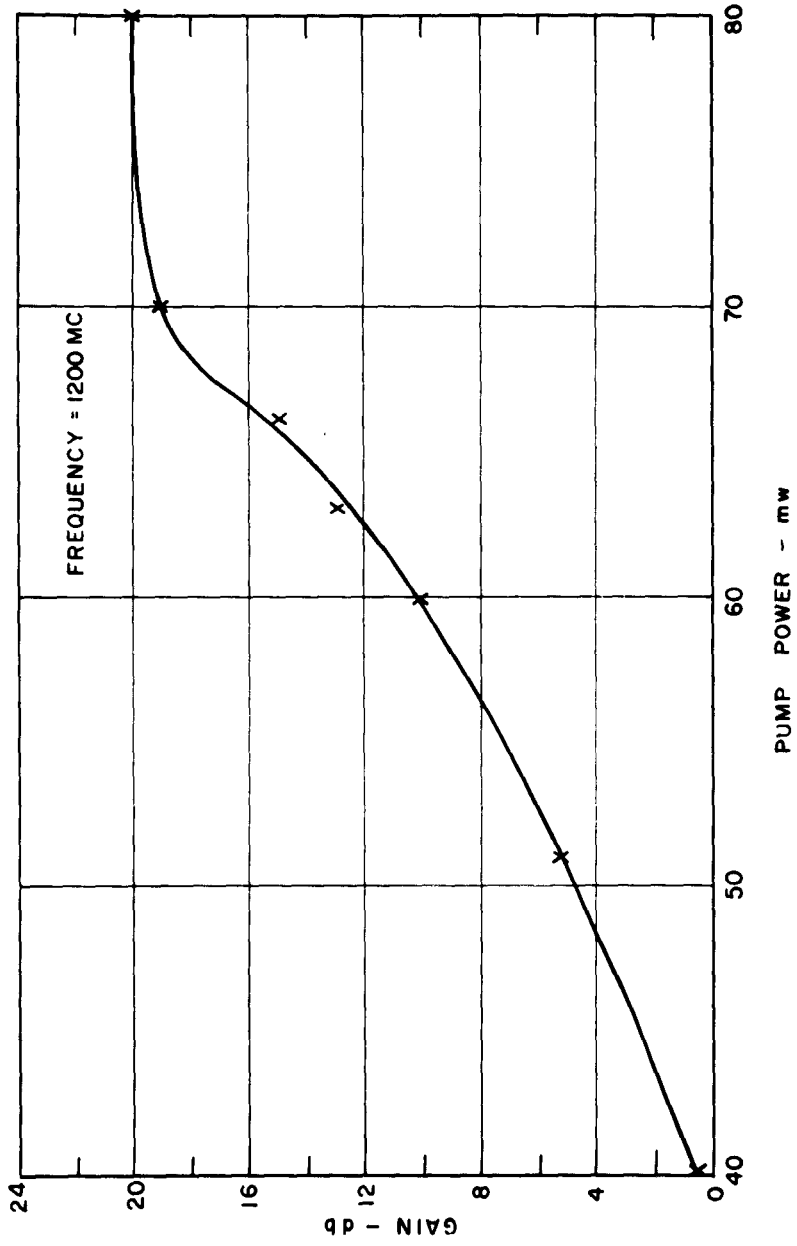

Fig. 13 — Gain of the modulator-demodulator amplifier versus pump power

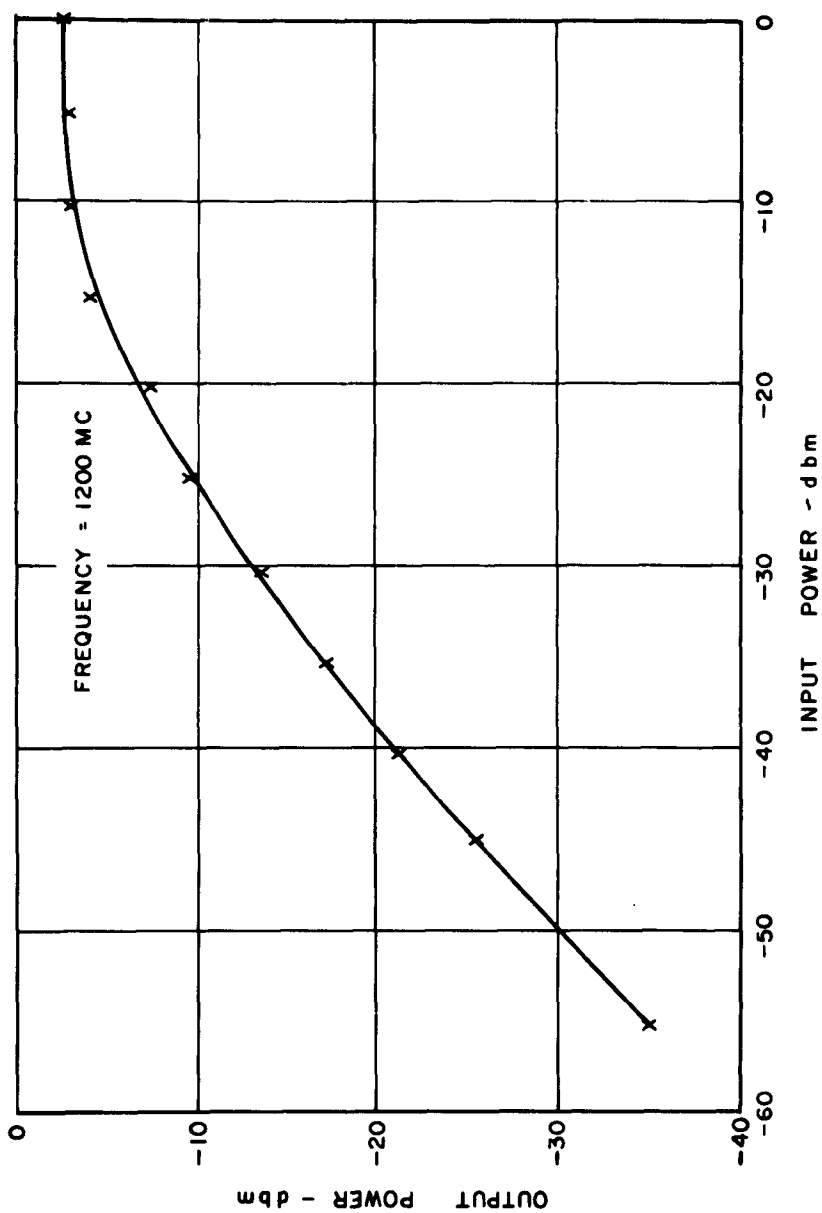

Fig. 14 — Output power of the modulator-demodulator versus input power

VII. RECOMMENDATIONS

The low-noise, L-band tunnel-diode amplifiers developed during this program should be scaled to S-band. The Electron Tube Division believes that tunnel-diode amplifiers that meet the following specifications can be built:

Frequency	3000 mc
Bandwidth	70 mc
Gain	greater than 10 db
Noise figure	less than 5 db
Size	compatible for use in phase-array antennas

Also, low-noise, S-band tunnel-diode down converters, in sizes compatible for use in phase-array antennas, should be developed. On the basis of the experience with L-band down converters gained from other programs, the Electron Tube Division believes that an S-band tunnel-diode down converter, which meets the following specifications, can be developed:

Signal frequency	3000 mc
Intermediate frequency	30 mc
IF bandwidth	2 mc
Noise figure	3.5 db

PART 2

DEVELOPMENT OF A VERY LOW NOISE, S-BAND TRAVELING-WAVE TUBE

PART 2

DEVELOPMENT OF A VERY LOW NOISE, S-BAND TRAVELING-WAVE TUBE

I. INTRODUCTION

Low-noise traveling-wave tubes with noise figures in the order of 6 - 10 db have been available in recent years and have given generally good performance as input amplifiers in the UHF through the X-band frequency ranges. The relatively high gain, good stability, and broadband capabilities of the traveling-wave-tube amplifier, coupled with the possibility of achieving improved noise performance in a miniaturized permanent magnet focusing package, has again emphasized the versatility of these devices in those applications where extremely low noise operation is not required.

This report describes the development of a traveling-wave-tube amplifier that has demonstrated a capability for very low noise operation in the S-band range of microwave frequencies.

II. OBJECTIVES

RCA proposed a ten-month program for the development and demonstration of a very low noise traveling-wave tube for operation in the S-band frequency range. The major requirements of the low-noise traveling-wave tube were as follows:

Frequency	2.7 to 3.5 kmc
Tube noise figure	2 db (max.)
Small-signal gain	25 db (min.)
Saturated power output	1 mw (min.)

VSWR	
Input	2/1 max.
Output	2/1 max.
Gain linearity	TBD
Phase linearity	TBD
Focusing	solenoid

Effort on this program was to be directed largely towards improving the noise figure performance of RCA's proved low-noise traveling-wave tube design, the RCA type 6861. This was to be done through an experimental electron gun improvement program supported by available theory. Theoretical work indicating new methods for achieving improved noise reduction in electron gun designs was to be investigated.

Major effort was to be directed toward the full utilization of theoretically possible noise-reducing mechanisms involving such factors as improved low-noise cathodes, large space-charge current densities, space-charge-depressed virtual cathodes, and the noise filtering or dampening effects of slowly drifting electron streams, to name but a few.

While the major effort on these feasibility studies was to center around the basic RCA type 6861 design, some exploratory work concerning a miniaturization of this design was also planned. The proposed developmental schedule for this program is given in Appendix A.

III. THE EXPLORATORY PHASE OF THE PROGRAM

The basic RCA type 6861 low-noise traveling-wave tube very nearly meets all the requirements of the required traveling-wave tube design except that of tube noise figure. Because of the apparent feasibility and facility of obtaining the desired objectives with a modified 6861 design, plus the general availability of parts and fabrication facilities for this design, emphasis was placed on this design approach for the exploratory phase of this program.

The RCA type 6861 tube uses a relatively high-impedance helix ruggedly supported by three ceramic rods that are firmly clamped at periodic intervals along the helix length. Coaxial-cavity type of input and output rf couplers are voltage coupler to antennas that terminate the tube helix. The 6861 design has a very low-loss rf circuit which contributes to the good noise performance consistently achieved with this tube. Figure 1 shows a cross section of the "bottle" for the 6861 tube.

A. Design Features of the RCA 6861 Tube

The basic features of the RCA type 6861 low-noise electron gun are shown in Fig. 2. In the cross-sectional view of this electron gun (Fig. 2a), the region between Grid No. 1 and Grid No. 2 may be considered as the beam-launching region and the region between Grid No. 3 and Grid No. 4 the beam-impedance transformer in the gun. Located in the region of Grid No. 2 is a section of the electron gun where the electron stream drifts for a considerable length at a

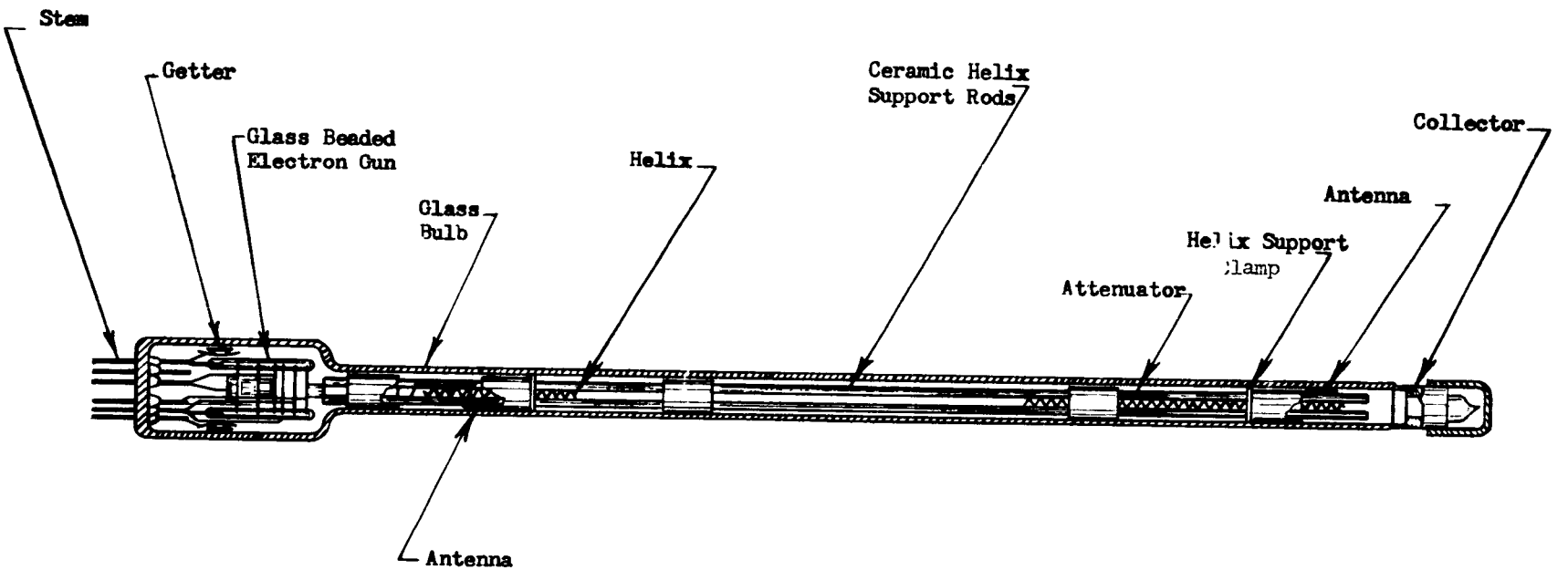

Fig. 1 — Cross section of the type 6861 "bottle".

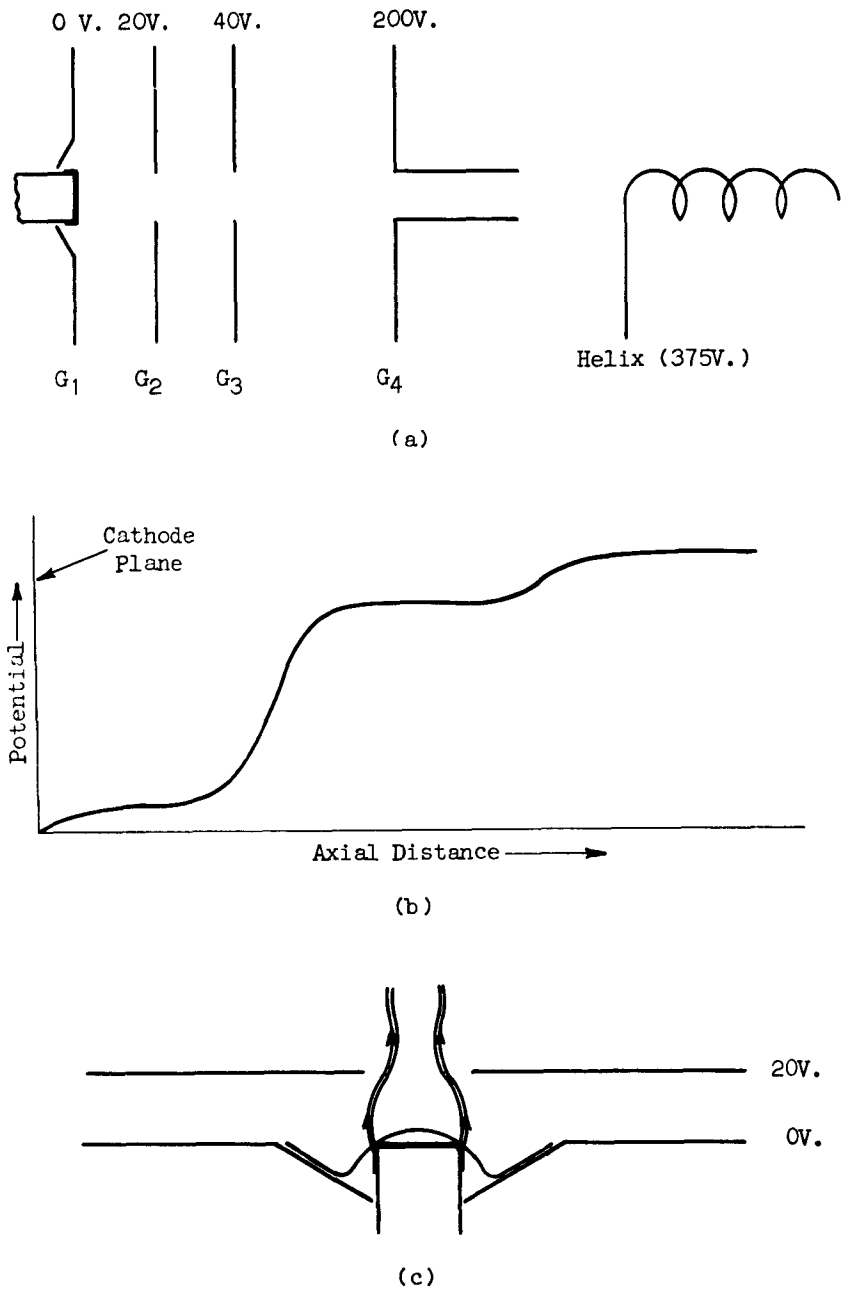

Fig. 2 – Basic features of the RCA Type 6861 low-noise electron gun. (a) Cross section of electron gun. (b) Beam-edge potential profile. (c) Beam launching characteristics.

relatively low velocity. This is pointed out more clearly in the approximate beam-edge potential profile shown in Fig. 2b.

The electron gun geometry, shown in Fig. 2c, was empirically adjusted so that optimum noise performance was achieved with the beam-forming element, Grid No. 1, operated at zero bias and the magnetic field at about 525 gausses. The position of the cathode in relationship to the shaped beam-forming element partly determines the configuration of a two-dimensional electric field at the cathode. This configuration is such that the potential profiles are distorted about the planar cathode in such a way that most of the cathode emission is from about a 5 mil width at the cathode periphery with current density diminishing rapidly in the direction of the tube axis. Thus, this electron stream can be considered to be essentially hollow in nature.

B. New Exploratory Tests

The exploratory studies made during this program have shown that the nature of the cathode coating and the beam-launching conditions in this region, especially with regard to (1) electric and magnetic field configurations and (2) the current densities used, were found to be of extreme importance in determining the ultimate noise performance of the tube. A theoretical discussion of the possible noise-reduction mechanisms which may be involved in this region, as well as an analysis of the experimental results which have been obtained, are treated at length in the Scientific Reports No. 1 and No. 2 which have been submitted as part of this program.

The exploratory investigations have also indicated that a definite improvement in tube noise performance could also be obtained through modifications in the beam-impedance transformation process. In this region, velocity fluctuations on the beam are small compared to the average velocity of the beam. However, the incorporation of lens effects in this region have shown a definite effect on the tube noise figure, which, under proper conditions, can be somewhat lower than that obtained with the more commonly employed exponential type of beam-impedance transformation. Noise-reduction effects due to the focal action of weak lenses, including the effects of aberrations in these lenses, have been postulated and considered, in part, in the Scientific Reports also. Much of the development effort in the latter stages of this program was aimed at taking advantage of these observed effects in revised multigrid low-noise electron gun designs.

During the exploratory phase, and continued throughout the development program, many design facets which could lead to improved rf performance, especially with regard to tube noise, were investigated and, in many instances, evaluated in actual tests. (See Appendix B.)

Some of the more important phases in this program will now be considered.

IV. THE DEVELOPMENT PHASE OF THE PROGRAM

The development phase of this program involved two aspects; (1) an optimum tube design, and (2) an optimum solenoid design.

A. Tube Development

The factors vital to the attainment of low-noise performance in traveling-wave tubes can be separated into four distinct regions in the tube structure as follows:

(1) The low-noise cathode
(2) The beam-launching region
(3) The beam-impedance-transformation region
(4) The beam-helix interaction region

The development portion of this program emphasized general design improvements in these areas, as well as the evaluation of relatively new techniques.

1. The Low-Noise Cathode. — The nature of the cathode is a prime factor in the determination of the ultimate noise figure of the traveling-wave tube. Strong supporting evidence was obtained for the premise that a high noise figure in an otherwise low-noise tube design, if not due to excess gas in the tube, is almost certainly due to excess noise velocity brought about by cathode non-uniformities. Tubes having such defective cathodes showed, in general, marked improvement in noise performance with the application of noise reducing techniques that, in theory, reduced excess noise velocities.

In view of the fact that the beam current in the low-noise electron gun designs considered in this program essentially originates from the cathode periphery, the physical nature of the cathode in this region was extensively investigated with regard to its effect on noise performance.

The cathodes were found to require a rather dense, homogeneous deposit of emitting material in this region, the coating thickness being in the order of 1 mil and the density in the order of 1.5 grams/cm^3. Meticulous care must be taken to protect this coating during all subsequent processing operations in order to develop a final active cathode surface which will provide adequate uniform emission at temperatures in the order of 600^{o}C.

The cathode periphery must be free of any physical defects, which could give rise to excess noise velocities, such as an excessively rough finish or razor sharp edges. Much effort was expended in determining the correct geometry for this cathode edge and the best means for obtaining it. Best noise performance was secured with cathodes having a 45^{o} bevel with a 1 to 2 mil flat at the cathode edge.

Matrix type of cathodes were investigated briefly. While the test data obtained was not conclusive, it appeared that noise-reduction mechanisms were effective with these cathodes also, with noise increases resulting only from the higher operating temperatures of these cathodes. Matrix cathodes were investigated primarily because of some concern of the higher cathode loading used in these low-noise developmental tubes. Subsequent sampling of tubes based on this development indicates that good tube life will be obtained from oxide cathodes.

2. <u>The Beam-Launching Region.</u> — The short region in front of the low-noise cathode, where fluctuations in electron velocities can be comparable to the average electron velocity, has proven to be a very fruitful area for reduction of the beam noise below that represented by the cathode temperature.

Techniques involving theoretical considerations, as depicted in the Scientific Reports, were pursued during the entire program. Emphasis was placed on the following techniques.

1. Crossed-field beam launching and focusing.
2. Low-velocity beam launching with electrostatic lens effects.
3. Created virtual cathodes using lens techniques.

Crossed-field launching and focusing effects in this beam-launching region have been postulated as the prime factors in beam noise reduction and have been considered in more detail in Scientific Report No. 2. Additional factors concerning this technique are given in the section devoted to the final tube design, since these techniques form the basis of the developmental tube design.

Low-velocity beam-launching techniques, possibly also involving the action of an electrostatic lens in the region of the cathode, have been investigated but not pursued since such techniques resulted in a smaller diameter, low-density electron stream, and thus, would require a new design for the slow-wave helix structure to obtain optimum results. These techniques have, in general, been pursued at other laboratories, and thus, further effort on this program would only amount to a duplication of this effort.

Attempts to create a new virtual cathode region, displaced some distance from the cathode potential minimum, by means of lens action, such as an Einzel type lens with highly depressed center electrode, proved to be impractical. The electron-mirror effects present were quite unstable and space-charge

noise-reduction effects, if present, were not positively observed. Therefore, only a limited effort was expended on these investigations.

3. The Beam-Impedance-Transformation Region. — In general, the low impedance of the beam near the cathode is smoothly transformed into the higher impedance required in the interaction region, consistent with minimizing any increase in noise in this process. This modified exponential method of impedance transformation is preferred because of its flexibility. This characteristic of flexibility is important, for in the final tube design the impedance transformation requirement must also be compatible with the establishment of a definite drift length for the electron stream following the crossed-field launching region. This will be considered in further detail in the section on the final tube design.

Beam impedance transformation involving what may be considered an equivalent to an Einzel type of lens in this region gave consistently better noise performance than the normal exponential type of transformation. This improvement was generally only in the order of 0.5 db with well-processed low-noise cathodes, but could be drastic in its effect on the high noise generated by poor cathodes, i.e., those cathodes generating excess noise velocities due to excessively rough oxide deposits. A typical example of the effect of lens-type transformation on noise performance is shown in Fig. 3.

Experimental data seem to confirm that geometrical optics are involved in this process of apparent noise reduction with the use of electrostatic

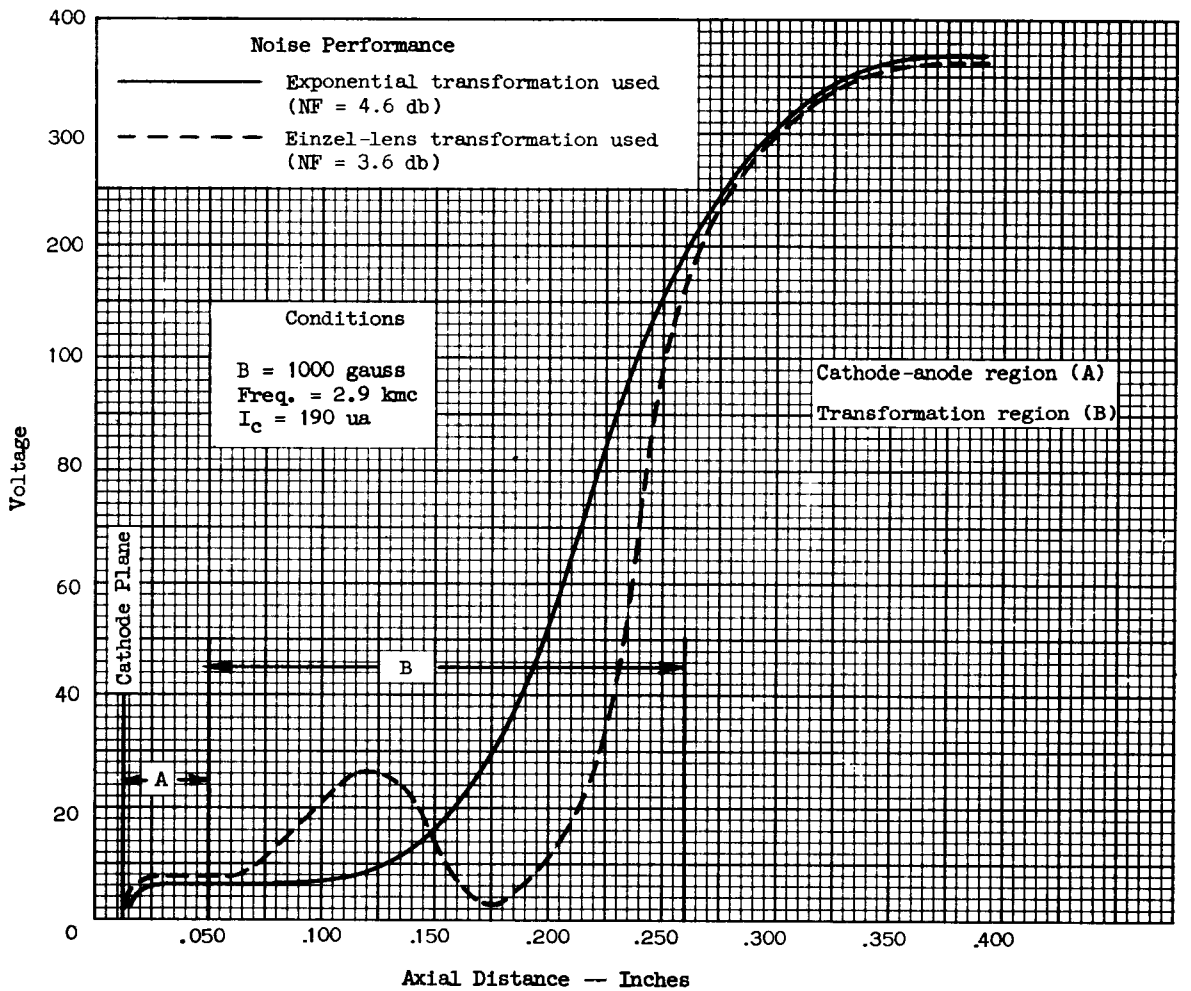

Fig. 3 — Comparison of beam-edge-potential profile of a tube using the exponential type of impedance transformation with that of a tube using the Einzel-lens type of transformation.

lenses as in the above example. The application of lens transformation techniques apparently also results in a noise-figure response which is more frequency sensitive; this implies that crossed-field effects may also be involved in this scheme. In addition, the effects of lens aberrations might also be involved in a process which could result in a reduction in the spread of axial electron velocities. However, the presence of what appears to be a simple weak lens structure may be much more complicated in its effect on basic tube noise. Similar structures have been postulated by other workers in the field in the past as affording different types of noise-reducing mechanisms.

While lens effects have proved useful in exploratory tubes operated in uniform-field solenoid tests, such effects proved somewhat critical in the special jump-field solenoid design. This may be due to the fact that the effects of the electrostatic lens were complicated by the radial component of magnetic field in this region which is developed by the jump-field solenoid design. Since corrective measures for this problem involved a redesign of the jump-field solenoid, lens effects were not included in the final design of the low-noise traveling-wave tube. In addition, these lens effects could complicate the redesign of this tube for permanent magnet focusing.

4. The Beam-Helix-Interaction Region. — Very low noise tube performance requires an optimum design of the interaction elements. This area has been adequately discussed in the literature and will not be elaborated upon here. In general, low-noise tubes are designed to optimize the interaction between

the wave and beam through minimization of the space-charge factor, QC, and a reduction of the loss factor, d, while maintaining the gain factor, C, reasonably high. These conditions are essentially met in the basic 6861 tube design.

Losses are reduced through an optimum helix design as well as use of low-loss helix supports. Some effort was expended on improved silver-plating techniques for the very low loss helices necessary in this tube design. The tungsten helices normally used did not always silverplate well and resulted in increased losses and even discontinuities (i.e., slivers, silver buildup, etc.) that caused rf reflections in the slow-wave structure.

Helices made of molybdenum wire were investigated. Molybdenum silverplated very well, either as straight wire, or as coiled helices. The evaluation of these molybdenum helices in finished tubes was complicated by gas effects (due to other causes) found in these tubes. However, past experience has shown that the noise performance is noticeably effected by the nature of the helix losses as indicated by the plating quality. Therefore, it can be expected that the use of well-plated molybdenum wire for the helices would result in a definite improvement in tube noise performance.

Electron gun-helix alignment was found to be very important in the developmental tube designs for several reasons. For example, the beam-launching noise-reduction techniques depend on radial symmetry for optimum effect. The transition of a highly confined hollow beam in the gun region to a quasi-Brillouin type of beam flow in the interaction region again requires radial

symmetry in this region and also a precise axial alignment. Otherwise, beam-skewing effects, whether due to magnetic defects or alignment defects, would result in excessive helix interception and possible noise degradations due to the release of helix-trapped gas molecules.

Several methods of improving the gun-helix alignment were investigated, all involving various methods of clamping the 3-rod helix structure to the electron gun drift tube. A slight modification to the basic method used in the standard 6861 tube design was found to be satisfactory in this regard. Gun-helix misalignment also complicates the determination of optimum noise performance since it may not be possible to focus such tubes at the optimum magnetic field condition (which may be of relatively low value).

For the terminal noise figure to remain low, and to be free of excessive fine structure, the coupling to the slow-wave structure must also be low in loss and show very low VSWR response. Precision helix winding techniques must also be used to minimize the possibilities of rf reflections. Effort on this program devoted to coupler studies has led to coupler designs which covered the required frequency range of 2.7 to 3.5 kmc with the VSWR's in this range not exceeding 1.3 to 1. The coupling losses over this same range, including cable and rf fitting losses, generally range between 0.3 and 0.4 db. Coupling losses were found to be, at times, much higher than this. Much of this loss was associated with poor fabrication of the coaxial cavities or the use of lossy 50-ohm transmission line.

A summary of experimental noise figure results for the exploratory tube is given in Appendix B.

B. Solenoid Development

The high order of magnetic field required for constraining the very high density space-charge beam used in low-noise electron gun designs dictated the use, at least for the feasibility phase of this program, of a solenoid as the source of this magnetic field. The use of solenoids not only enables the generation of high-intensity magnetic fields, but also simplifies the problem of shaping and adjusting the magnetic field to meet the requirements for optimum focusing and noise performance.

Much of the experimental data taken during this program was obtained with operation of the low-noise traveling-wave tube in a relatively uniform magnetic field. This mode of operation, generally used with most low-noise tube designs, permits a highly-confined type of beam flow from the cathode to the collector.

Such a confined beam flow, originating from the divergent launching of a quasi-hollow beam at the cathode, is characterized by strong scalloping effects with beam flow down the interaction region of the tube. As a result of this scalloping action, the tube gain and power output drop sharply with frequency since the beam-helix interaction reduces with frequency. This is seen in the small signal gain curve for the RCA type 6861 tube shown in Fig. 7.

To improve the gain and power output characteristics of the low-noise traveling-wave tube, theoretical studies had indicated that it might be possible to go from highly confined beam flow in the low-noise electron gun region to a quasi-Brillouin type beam flow in the interaction region. This mode of operation could improve the stability of the hollow beam and improve beam-helix interaction through a reduction in beam scalloping effects. In addition, the proposed operation could result in a slight increase in the mean diameter of the stabilized hollow beam.

Effort expended on this program has shown that such a mode of operation was not only feasible, but also highly desirable.

A typical magnetic field configuration, characteristic of this mode of operation, is shown in Fig. 4. The electron gun is operated in region A, a region of relatively high and uniform magnetic intensity. In the transition region, the tapering of the magnetic field results in a radial magnetic field component of proper value which changes the beam flow from a highly confined type beam flow in region A, to a quasi-Brillouin type of beam flow in the interaction region, B.

A solenoid design based on this mode of operation has been developed for the final tube design and is described in the next section.

V. THE FINAL TUBE AND SOLENOID DESIGN

The exploratory phase of this development program has indicated that a tube design incorporating a crossed-field noise-reduction mechanism near the

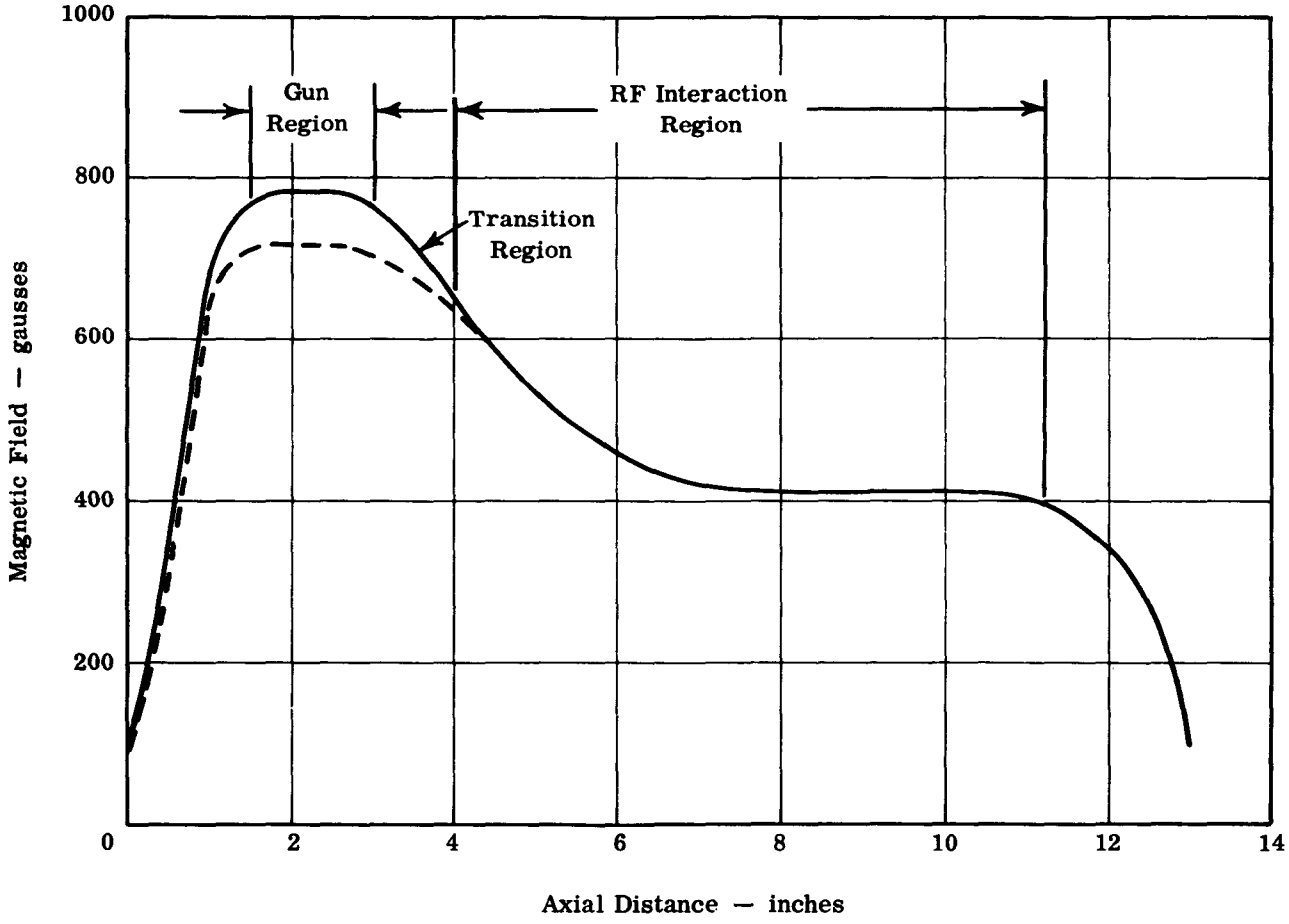

Fig. 4 — Magnetic field configurations for a typical jump-field type of focusing solenoid.

cathode and a lens type of beam impedance transformation would be best capable of achieving the lowest noise operation. However, the present design for the jump-field type of focusing solenoid has the radial component of magnetic field falling near this lens region. Therefore, the additional cross-field effects in this region has deleterious effects on this mode of operation. These effects were not observed during exploratory tests in a uniform field solenoid. Rather than redesign the jump-field solenoid at this late stage of the program, the lens features were eliminated from the final tube design.

A. The Final Tube Design

The final tube design is a modified version of the RCA type 6861 design considered earlier in this report. Essentially the same slow-wave structure and coupling systems are used as were present in the original prototype, but some design modifications have resulted in reduced losses and a much improved VSWR response.

The major modifications occur in the low-noise electron gun and consist of physical changes as well as differences in operating parameters. The physical modifications were all directed towards improving the beam-launching characteristics of the design and is based upon noise-reduction effects largely attributed to optimized crossed-field effects in the region of the low-noise cathode. Operating parameters were adjusted to values which satisfy the four general requirements in the low-noise electron gun developed on this program. Typical operating voltages for the new developmental tube design are shown in Fig. 5a. It is also

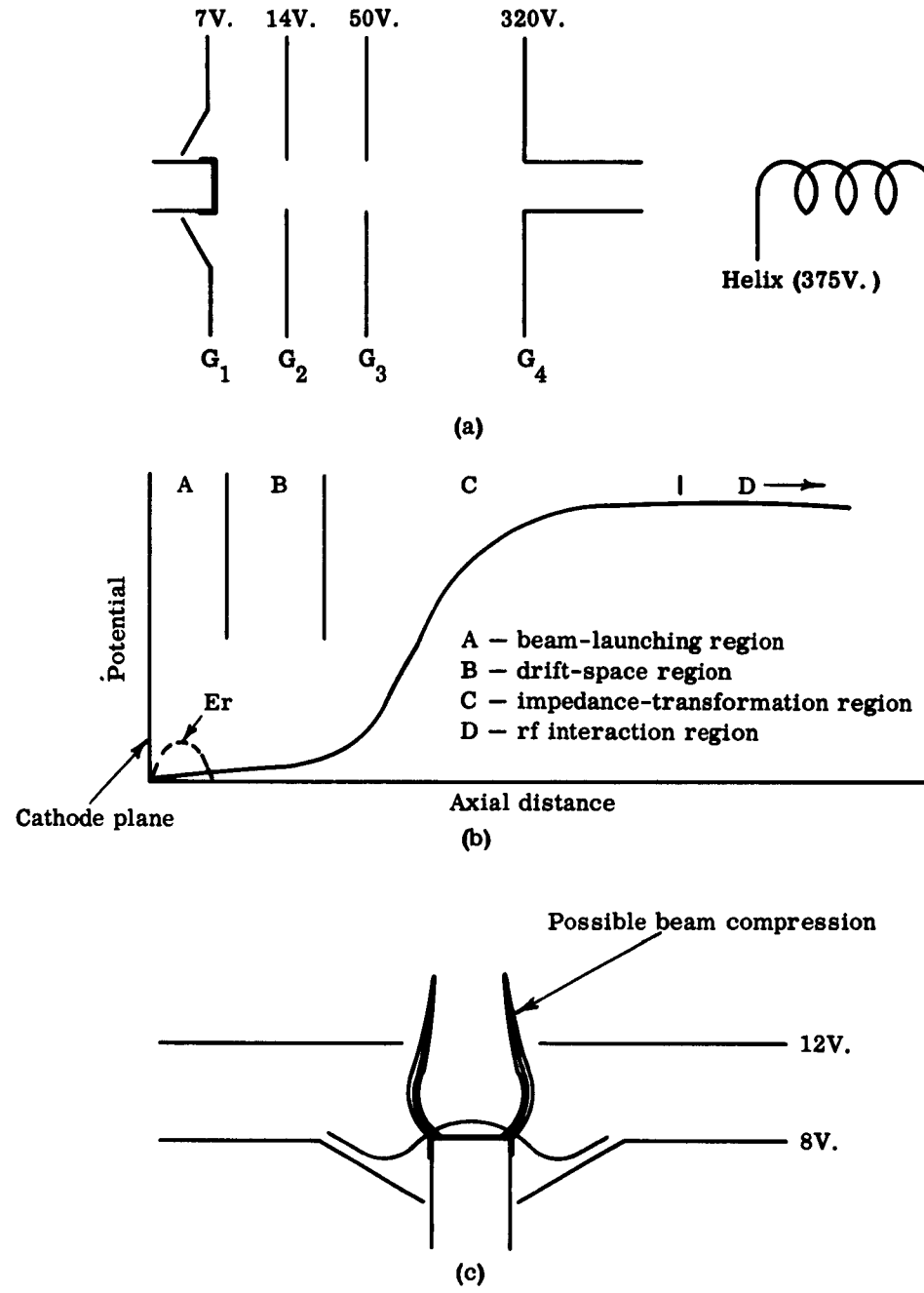

Fig. 5 — Basic features of the electron gun for the very low noise traveling-wave tube. (a) Cross section of the electron gun. (b) Beam edge potential profile. (c) Beam-launching characteristics.

possible for this design to operate with grid No. 4, helix and collector, all at the helix potential with but a slight increase in overall noise performance.

The fundamental features for this low-noise electron gun design are illustrated in the approximate beam edge potential profile shown in Fig. 5b. These characteristics are: (1) a crossed-field region near the cathode, A, (2) a low-potential, long-drift-length region, B, and (3) the modified exponential beam-impedance-transformation region, C. Figure 5c shows the feature of beam compression, which is believed possible in the trochoidal launching of the electron stream in the crossed-field region between grids No. 1 and No. 2. Such compression would enhance noise-shielding effects due to a higher beam space-charge density in this region.

B. The Final Solenoid Design

The drastically improved gain and power output characteristics achieved with the jump-field solenoid focusing scheme, with no degradation in noise performance, strongly favored use of this scheme with the final tube design. Figure 6 shows the basic features of the final solenoid design which incorporates the jump-field magnetic characteristics. The solenoid is approximately 5" in height, 15-1/2" in overall length, and weighs less than 30 lbs. The solenoid is capable of providing up to 1000 gausses in the gun-field region with use of adequate forced-air cooling. The normal operating point for this solenoid at S-band frequencies is at about 800 gausses for the gun field. Under these conditions, the solenoid requires about 82 volts at 2.25 amperes for a solenoid power dissipation of about

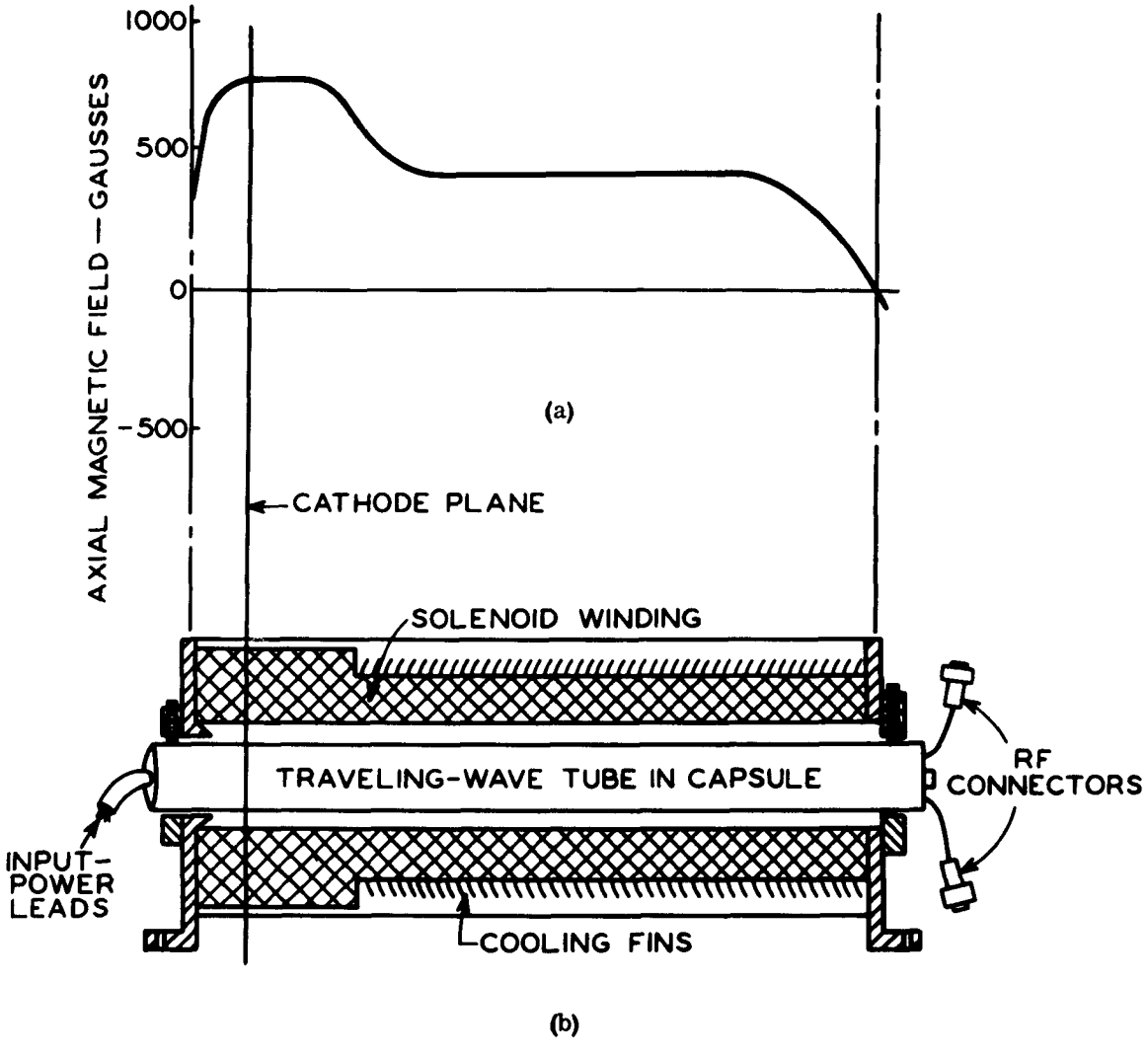

Fig. 6 — Focusing scheme for the very low noise traveling-wave tube. (a) Magnetic field configuration. (b) Encapsulated tube shown with a cross section of the jump-field solenoid.

185 watts. With the ambient temperature at about 40°C, a forced-air flow of approximately 120 cfm should be directed against the gun field of the solenoid. The solenoid is capable of safe performance under these conditions up to a maximum ambient temperature of about 65°C.

C. Characteristics of Final Tube Design

The final tube design, when operated in the jump-field solenoid design, has greater than 25 db small-signal gain and saturated power outputs in the order of 2 milliwatts. The 6861 tube design generally provides less than 25 db small-signal gain and saturated power outputs in the order of 1 milliwatt. The tube noise figure for the prototype 6861 was in the order of 6 db; the developmental tube noise figures are in the order of 3-4 db, with one tube showing a noise figure in the order of 2.5 db. This particular tube had an exceptionally well fabricated and processed low-noise cathode. Typical performance characteristics for the developmental tubes are shown in Fig. 7.

Sampling of tubes based on this design has shown that these tubes are capable of approximately 33 db gain and 3 to 4 mw of saturated power output, with tube noise figures remaining in the order of 3.5 to 4.0 db.

Reduction of the final tube design to a miniaturized version was not possible during the term of this program due to late delivery of the special glass required.

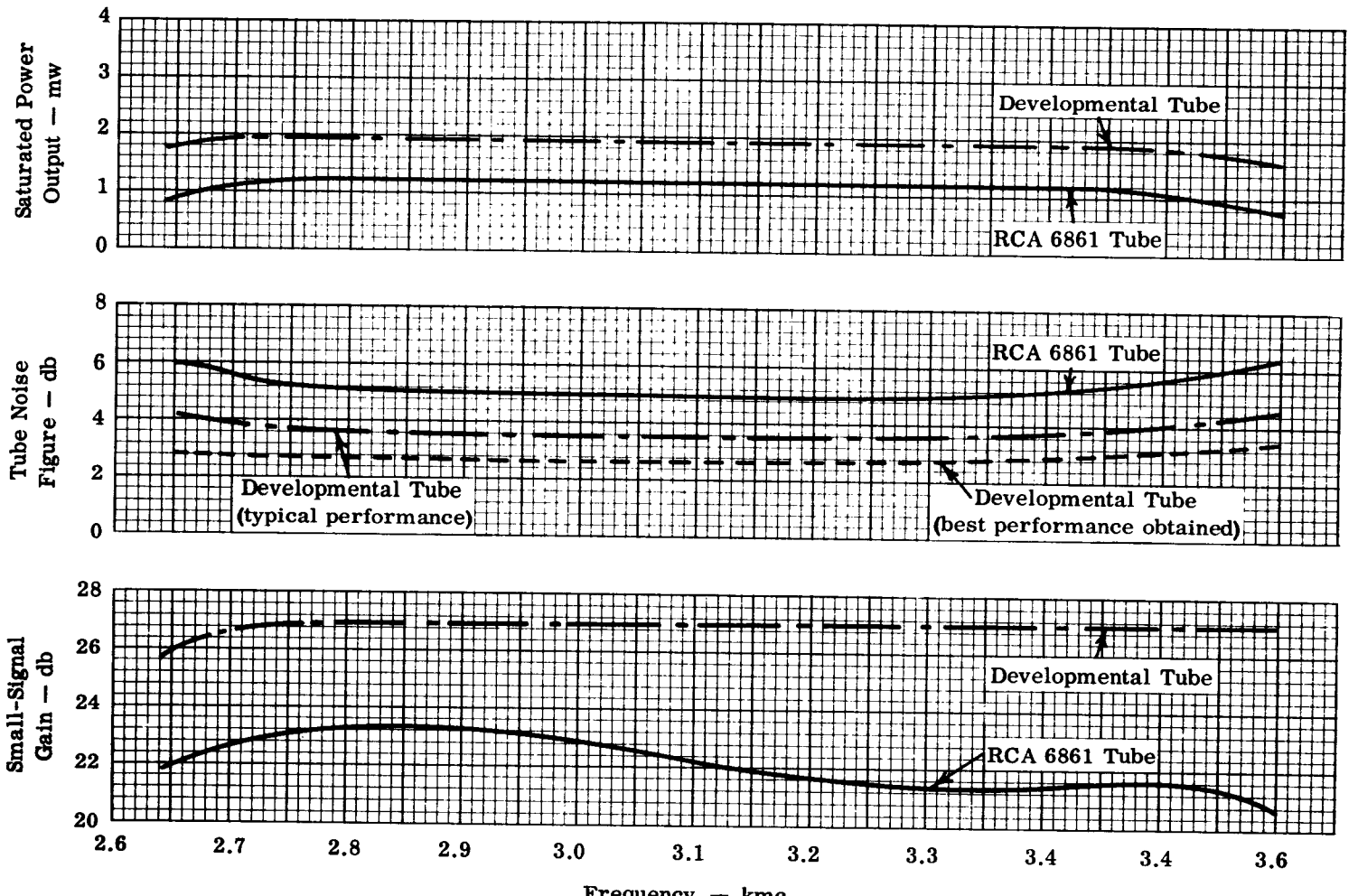

Fig. 7 — Comparison of the rf performance of the RCA 6861 traveling-wave tube with that of the very low noise developmental tube. (Saturated power output, tube noise figure, and small-signal gain versus frequency.)

VI. CONCLUSIONS

The main objective of the program outlined in this report was to determine the feasibility of designing a low-noise traveling-wave tube capable of higher gain and power output at much lower noise figures than were hitherto available. The 25 db (minimum) gain and 1 mw (minimum) saturated power output requirements were not considered severe and were readily met during the developmental phase of this program. The objective of a 2-db (maximum) tube noise figure which was not attained was found to require additional advances in the state-of-the-art in the form of new technical and design approaches to be accomplished.

Pursuance of a heuristic approach to the problem of noise reduction in electron beams has led to some interesting experimental results which, in the final analysis, could extend the noise theory for these devices. While the objective of a 2-db (maximum) tube noise figure was not achieved during this program, extrapolation of some of the experimental results obtained indicates that tube noise figures in the order of 1.5 - 2.0 db may be feasible. The best tube noise performance actually observed was in the order of 2.5 db. This performance was achieved with a very carefully fabricated and processed low-noise cathode.

VII. RECOMMENDATIONS

Design approaches leading to the development of a very low noise S-band traveling-wave tube design have been pursued during this program. Further refinements in the low-noise cathode fabrication and processing techniques, plus some refinements in the geometry of the beam-launching region of the low-noise

gun, can be expected to lead to tube designs having reproducible tube noise figures in the order of 2.0 - 2.5 db. Somewhat better noise figures may be expected with a lens type of beam impedance transformation, but such a feature would complicate a periodic-permanent-magnet design for this tube. In addition, experimental data indicate that a tube design using lens transformation would be frequency sensitive, i.e., relatively narrow band in operation.

Reduction of tube noise figures to levels below 2.0 db require (1) the evolution of a more efficient beam cooling or noise-extracting technique, and/or (2) further development of the noise filtering or dampening effects of high space-charge current densities in the electron stream.

Of course, the possibility always exists for the development of some radically different approach to the problem of noise reduction in beam type devices. The approaches followed on this development program were used largely because they lent themselves easily to experimental verification. In addition, these techniques can be adapted to an all-permanent-magnet focused package design. Subsequent limited sampling of tubes using this basic design has shown a high order of reproducibility in both operating parameters and rf characteristics.

APPENDIX A

DEVELOPMENTAL SCHEDULE

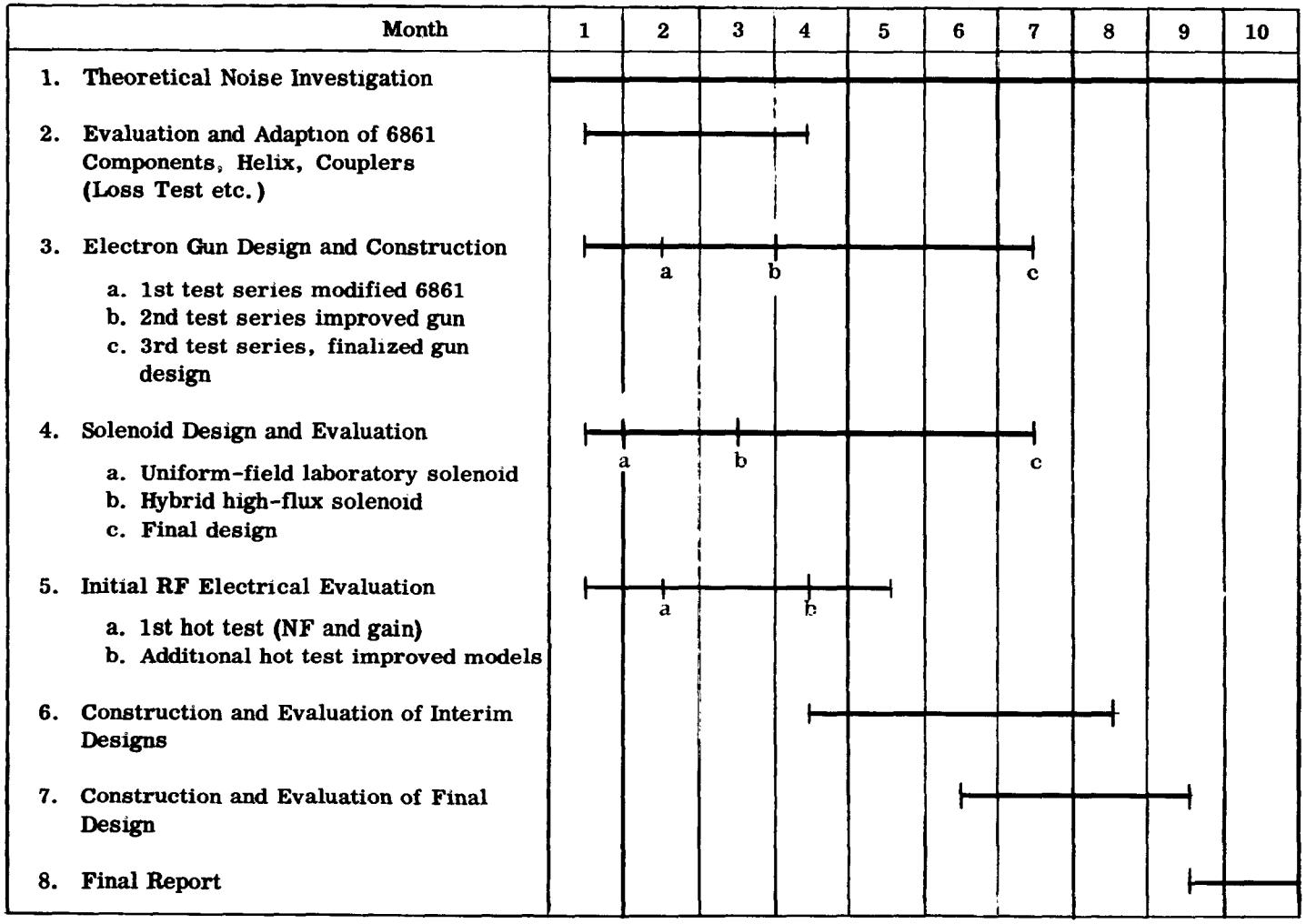

APPENDIX B

EXPERIMENTAL TUBE DATA

This appendix contains the data compiled from tests on tubes fabricated during this program. The data tabulated in Table I give the lowest noise figures that were obtained in each tube. The specific frequency, or frequency band, and the magnetic field strength at which these noise-figure values were obtained are also shown. Table II gives the optimum operating conditions for both the final developmental tube and the solenoid for S-band and L-band operation. The rf performance characteristics in both frequency bands are also indicated.

Six curves (Figs. 8 through 13) that describe tube performance as a function of frequency, magnetic field, or beam current are also included herein

TABLE I

SUMMARY OF PERFORMANCE FOR
TUBES FABRICATED DURING THIS PROGRAM

Tube No.	Design Features	Freq. (kmc)	Best NF (db)	Magnetic Field (gausses)	Remarks
F-1	hollow-cathode	2.9-3.3	3.9	700	broken in tests
F-2	2-mil cathode bevel	---	---	---	shrunk at exhaust
F-3	2-mil cathode bevel	2.6-3.0	2.6	850	heater opened in tests
F-4	10-mil cathode bevel non-plated helix test	2.8	4.9	725	very lossy helix
F-5	10-mil cathode bevel	2.8	4.7	1100	poor focus
F-6	5-mil cathode bevel	---	---	---	shrunk at exhaust

TABLE I (CONT.)

Tube No.	Design Features	Freq. (kmc)	Best NF (db)	Magnetic Field (gausses)	Remarks
F-7	5-mil cathode bevel	2.7-3.0	3.4	825	tube developed gas
F-8	3-mil cathode bevel	---	---	---	shrunk for open weld in gun
F-9	3-mil cathode bevel	2.8	4.0	750	very gassy tube
F-10	matrix cathode	2.3	5.0	825	900°C cathode
L-1	3-mil cathode bevel in L-band test	1.4	4.0	525	low insertion loss, gain unstable
L-2	3-mil cathode bevel in L-band test	1.4	---	---	shrunk at exhaust
H-1	close-spaced aperture multigrid gun test	2.8	3.2	850	2-mil cathode bevel
H-2	lens-created virtual cathode test	---	---	---	very gassy tube
H-3	lens-created virtual cathode test	---	---	---	shrunk at exhaust
H-4	wide-spaced aperture multigrid gun test	2.8	3.1	660	2-mil cathode bevel
H-5	wide-spaced aperture multigrid gun test	2.9	3.4	660	5-mil cathode bevel
H-6	wide-spaced aperture multigrid gun test	2.7	3.8	1100	10-mil cathode bevel
H-7	wide-spaced aperture multigrid gun test	2.7	3.8	700	5-mil cathode bevel
H-8	lens-created virtual cathode gun test	---	---	---	shrunk loose cathode
H-9	wide-spaced aperture multigrid gun test	2.7	4.2	600	very gassy tube
H-10	lens-created virtual cathode gun test	---	---	---	evaluation incomplete
H-11	lens-transformation gun test	2.7	3.5	1500	poor focus

TABLE I (CONT.)

Tube No.	Design Features	Freq. (kmc)	Best NF (db)	Magnetic Field (gausses)	Remarks
H-12	lens-transformation gun test	---	---	---	broken in tests
H-13	lens-transformation gun test	2.8	4.5	800	very gassy tube
H-14	moly helix test	---	---	---	evaluation incomplete
H-15	moly helix test	---	---	---	evaluation incomplete
H-16	lens-transformation gun test	---	---	---	shrunk at exhaust
H-17	lens-created virtual cathode test	---	---	---	evaluation incomplete
H-18	wide-spaced aperture multigrid gun test	2.6-3.0	3.1	1125	tested in jump-field solenoid

TABLE II

OPERATING CONDITIONS AND TYPICAL PERFORMANCE CHARACTERISTICS OF THE DEVELOPMENTAL TUBES[1]

Parameter	S-Band Operation[2]	L-Band Operation[3]
	Tube Operating Conditions[4]	
Grid No. 1 voltage	7 volts	-2 volts
Grid No. 2 voltage	14 volts	22 volts
Grid No. 3 voltage	50 volts	35 volts
Grid No. 4 voltage	320 volts	135 volts
Helix voltage	375 volts	170 volts
Helix current	less than 0.5 μa	less than 0.5 μa
Collector voltage	800 volts	500 volts
Collector current	200 μa	200 μa

TABLE II (CONT.)

Parameter	S-Band Operation[2]	L-Band Operation[3]
	Solenoid Operating Conditions	
Magnetic field	jump field which tapers from 750 to 430 gausses	jump field which tapers from 560 to 430 gausses
Voltage	70 volts	60 volts
Current	2.3 amperes	1.8 amperes
Input power	160 watts	110 watts
	RF Performance	
Small-signal gain	30 to 35 db	30 to 35 db
Saturated power output	2 to 3 mw	1 to 2 mw
Tube noise figure	3 to 4 db	3 to 4 db

Notes:

1. Also includes data from RCA sample tubes.
2. Helix similar to that of the RCA 6861.
3. Helix similar to that of the RCA A-1056.
4. Heater for all tubes operates at approximately 3.7 to 4.0 volts, at 0.60 to 0.65 amperes, and is adjusted for best noise performance.

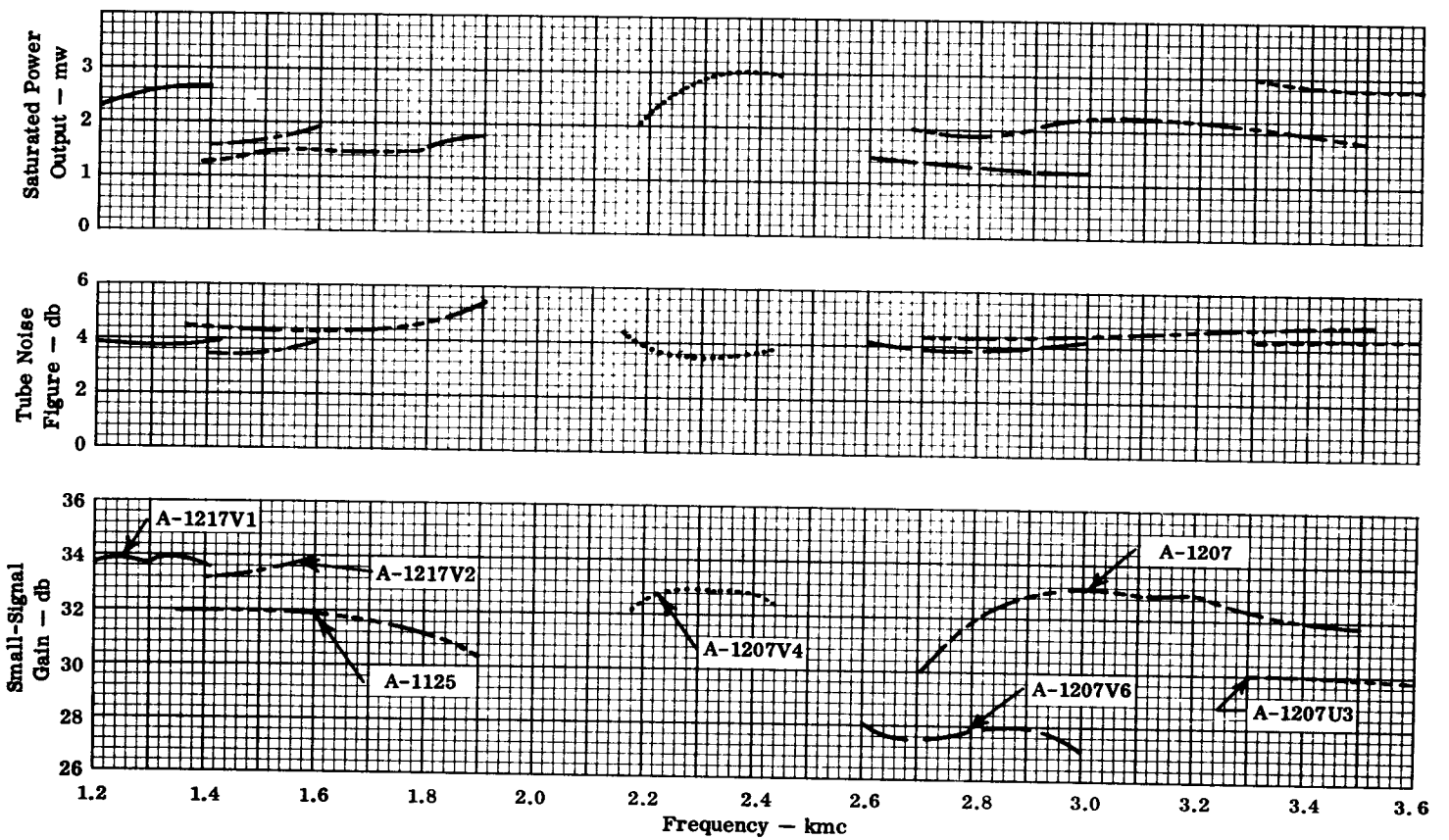

Fig. 8 – Typical rf performance of several RCA sample tubes. (Sample-tube design was based on that of the developmental tubes.)

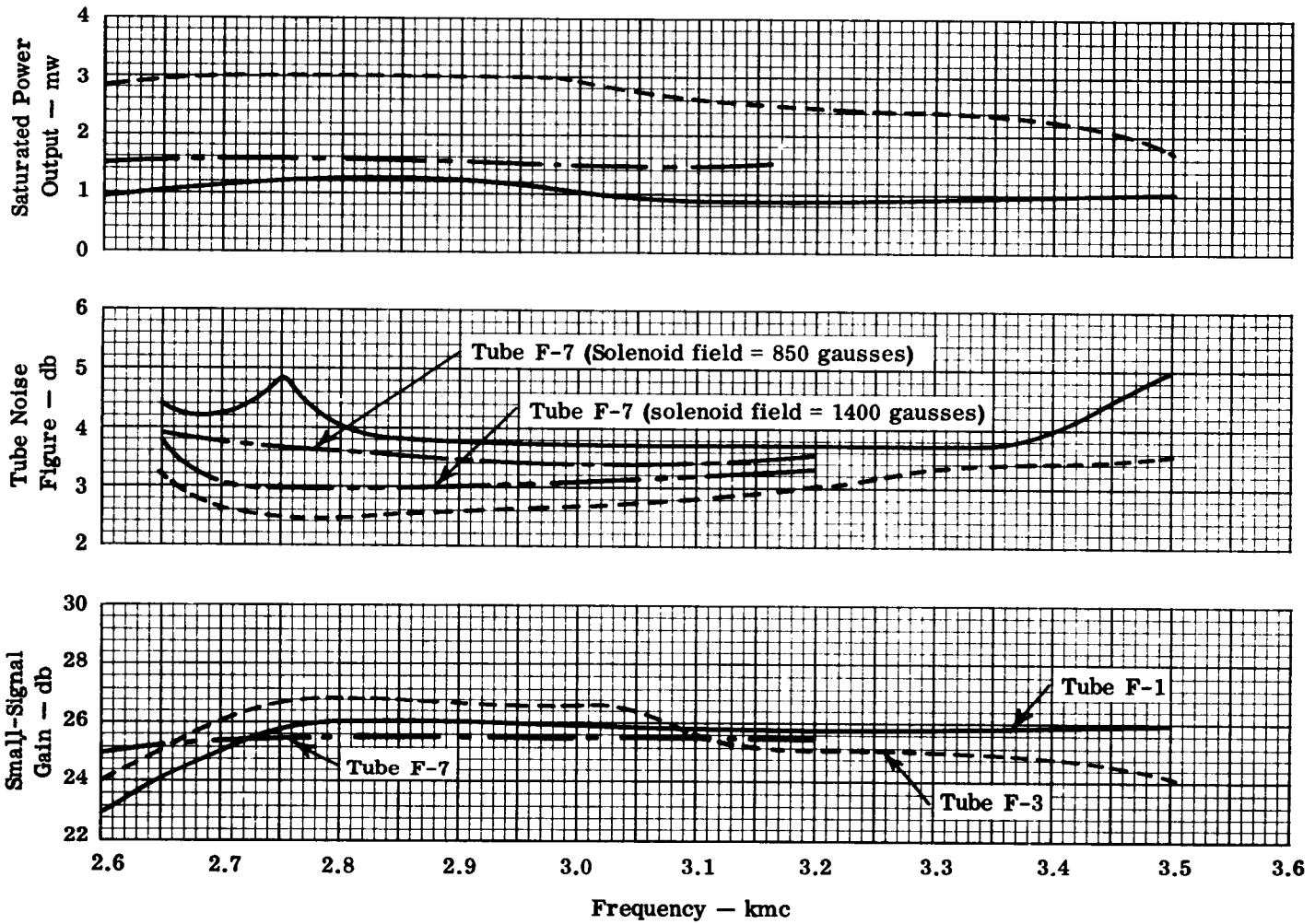

Fig. 9 — RF performance of three developmental tubes operated in a uniform-field solenoid.

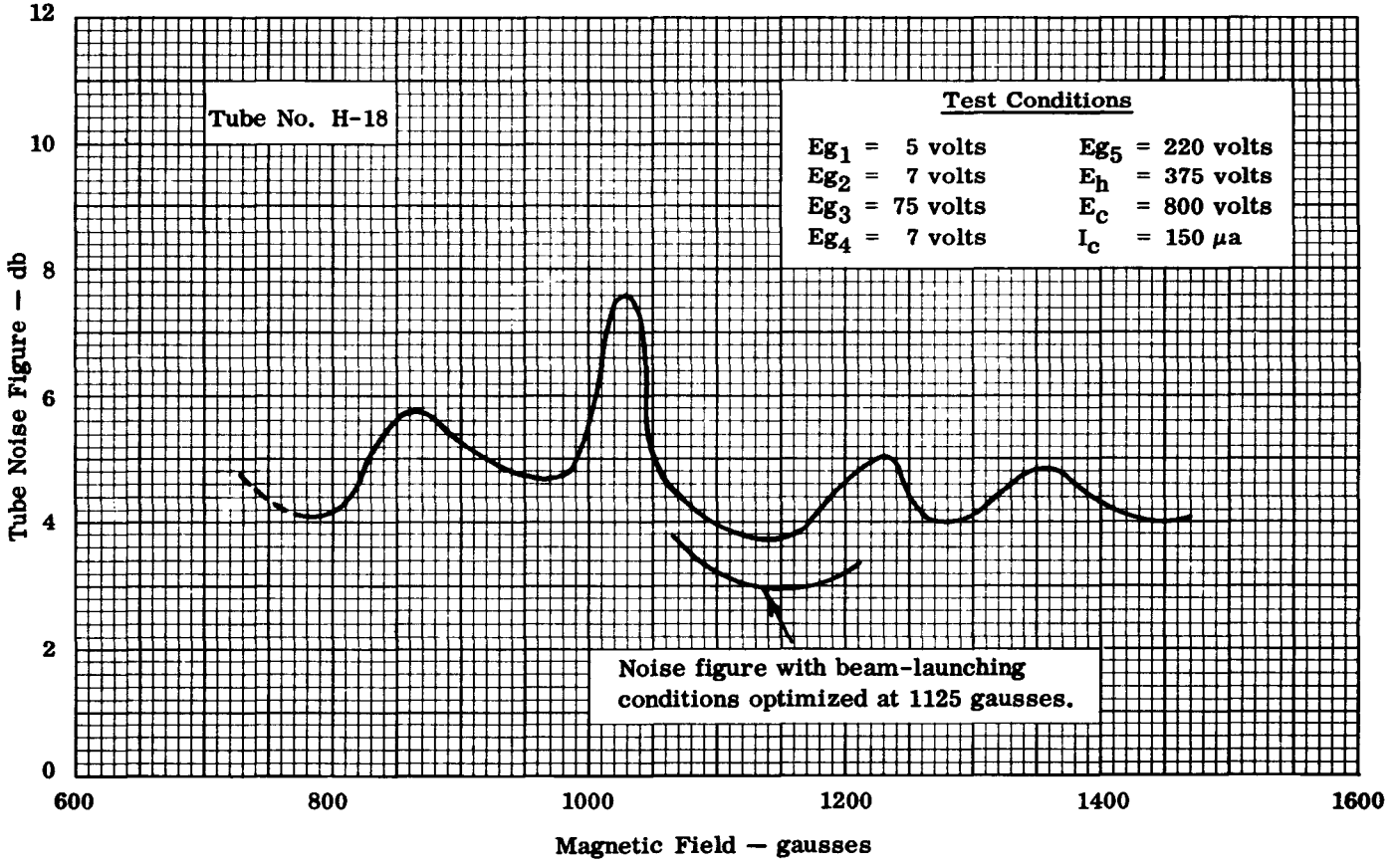

Fig. 10 — Tube noise figure as a function of the magnetic field for a lens type of tube operated at 2.7 kmc in the jump-field solenoid under fixed beam-launching conditions.

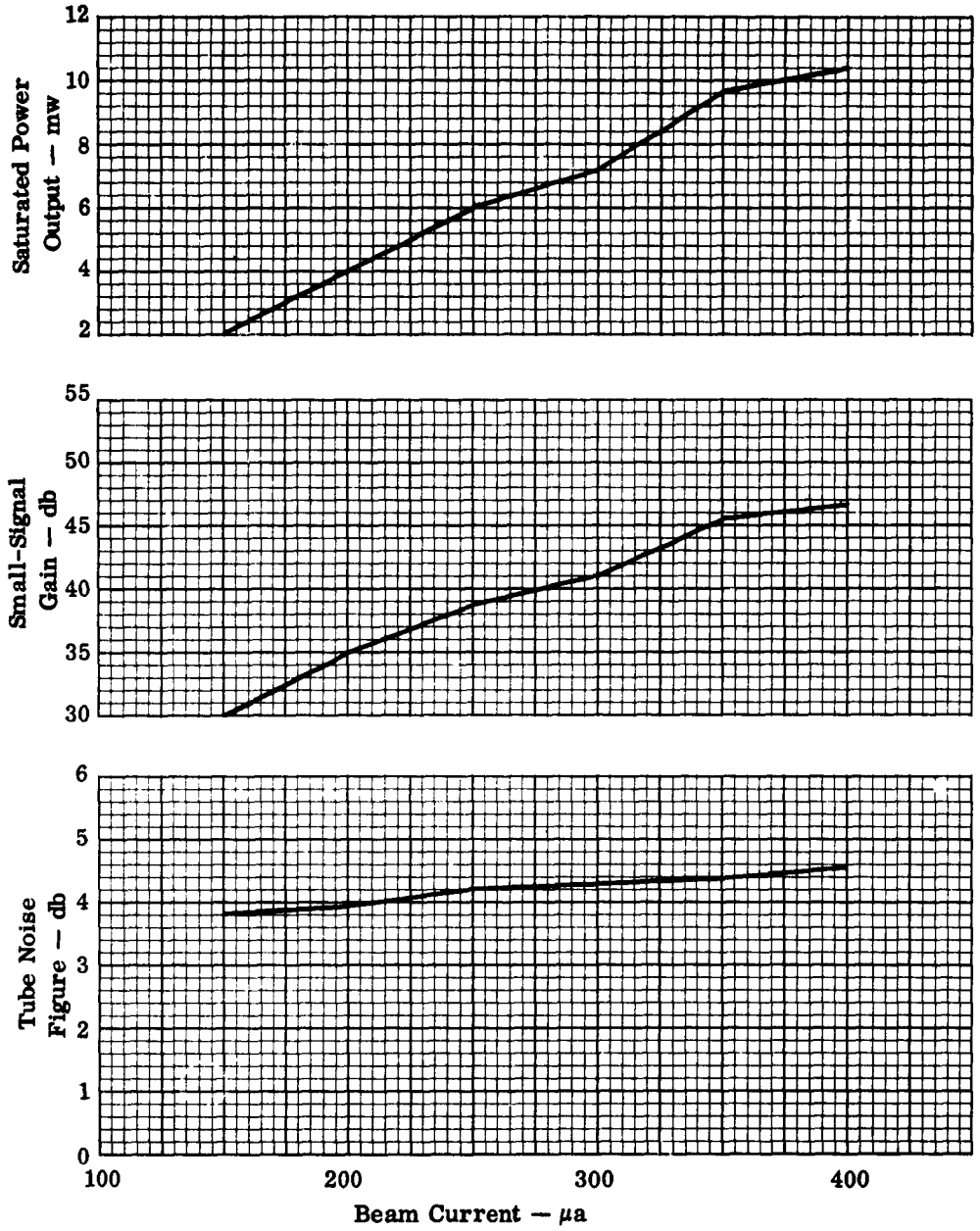

Fig. 11 — Saturated power output, small-signal gain, and tube noise figure as a function of beam current for a developmental tube operated at 2.8 kmc.

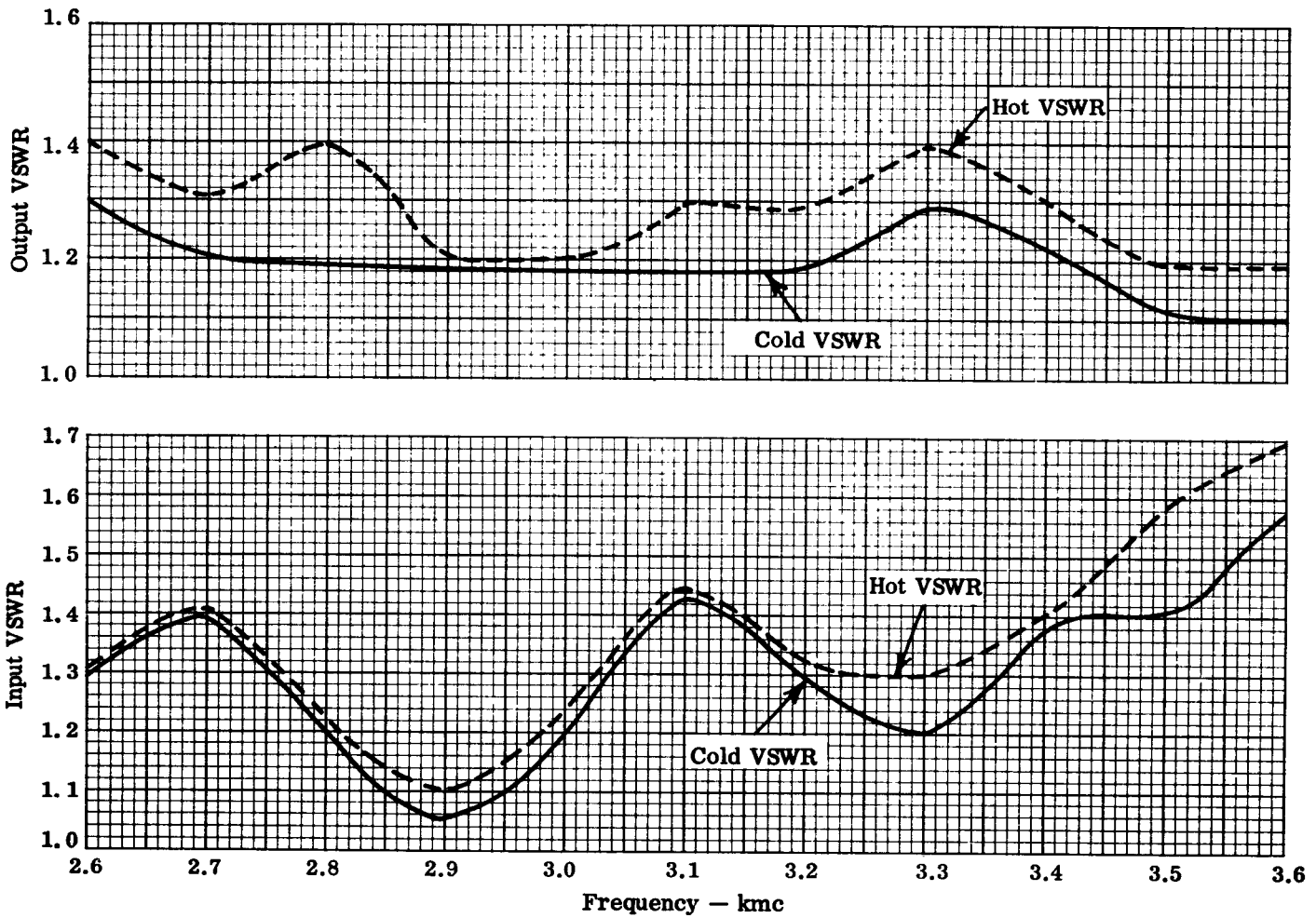

Fig. 12 — Typical VSWR versus frequency response for a developmental tube.

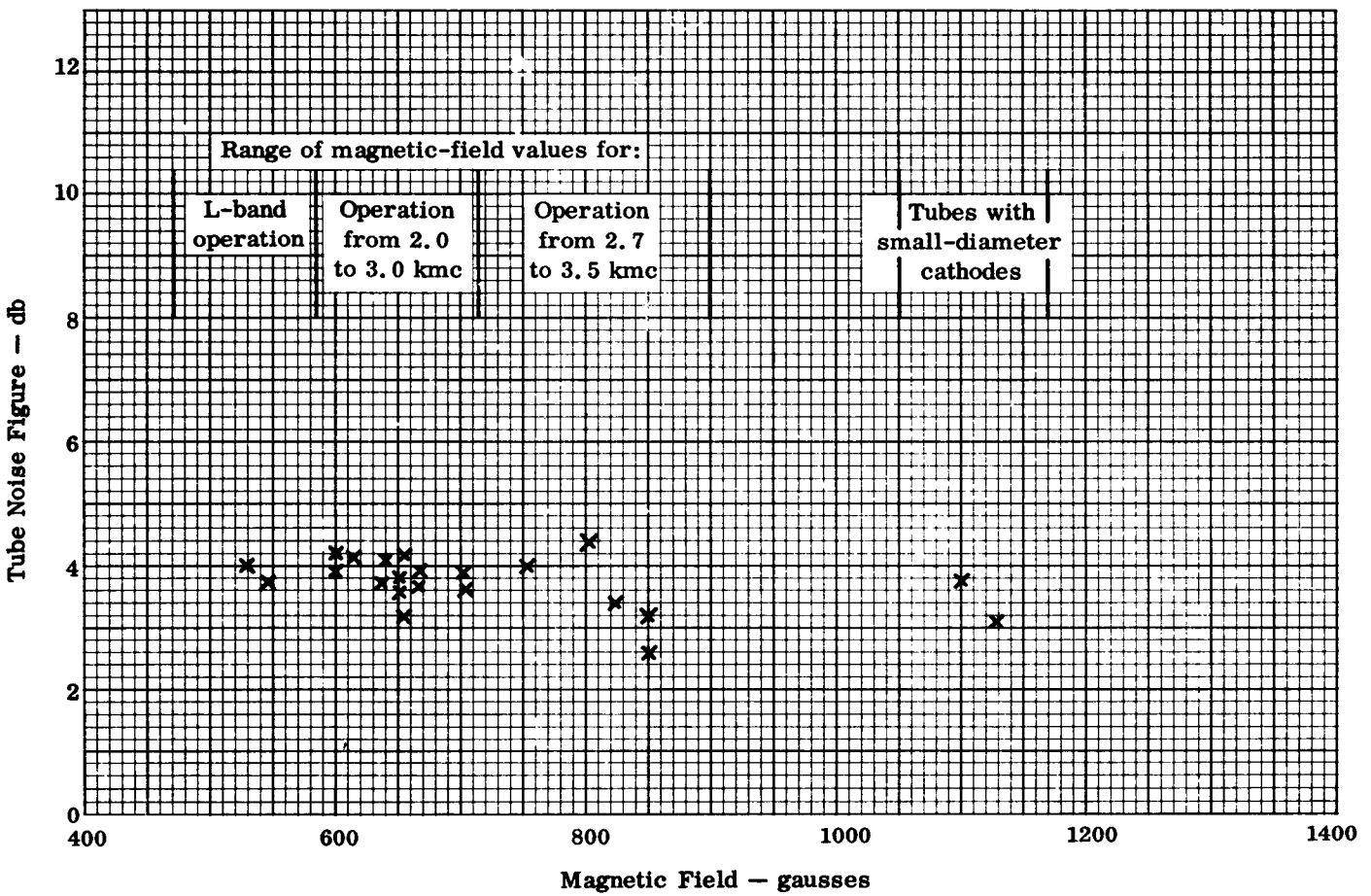

Fig. 13 — Noise figures versus magnetic field for a number of developmental and sample tubes.

APPENDIX C

NOISE-FIGURE MEASUREMENTS

Noise figure is proportional to the amount of noise added by the traveling-wave tube to the original signal-noise ratio (assuming signal and noise receive the same tube gain). Therefore, the simplest method of measuring noise figure is to add an equal amount of noise at the traveling-wave tube input to double the traveling-wave tube output noise signal indicated on a display meter. The basic equipment to perform these functions is shown schematically in Fig. 14. In this method, the noise of the argon-bulb noise source (A) as reduced by the precision attenuator (B), is added to the traveling-wave tube noise to double the traveling-wave tube output as measured by receiver (D). A 3-db if attenuator in receiver (D) is then inserted between the tube and the indicator to provide the same reading as from the traveling-wave tube noise itself minus the 3-db attenuator. The NF is then the NF of the noise source minus the precision rf attenuator loss.

More precise NF measurements can be made by using the standard Y factor procedure utilizing argon noise sources. The set-up shown in Fig. 14 can be used except that normally the argon noise source feeds directly into the traveling-wave tube under test (attenuator (B) is not used). The tube under test is adjusted for minimum noise output as indicated by the power-sensitive meter in the microwave receiver unit. (Note: Noise source off.) A known amount of noise (from the calibrated argon-bulb noise source) is then added to the tube input. The meter

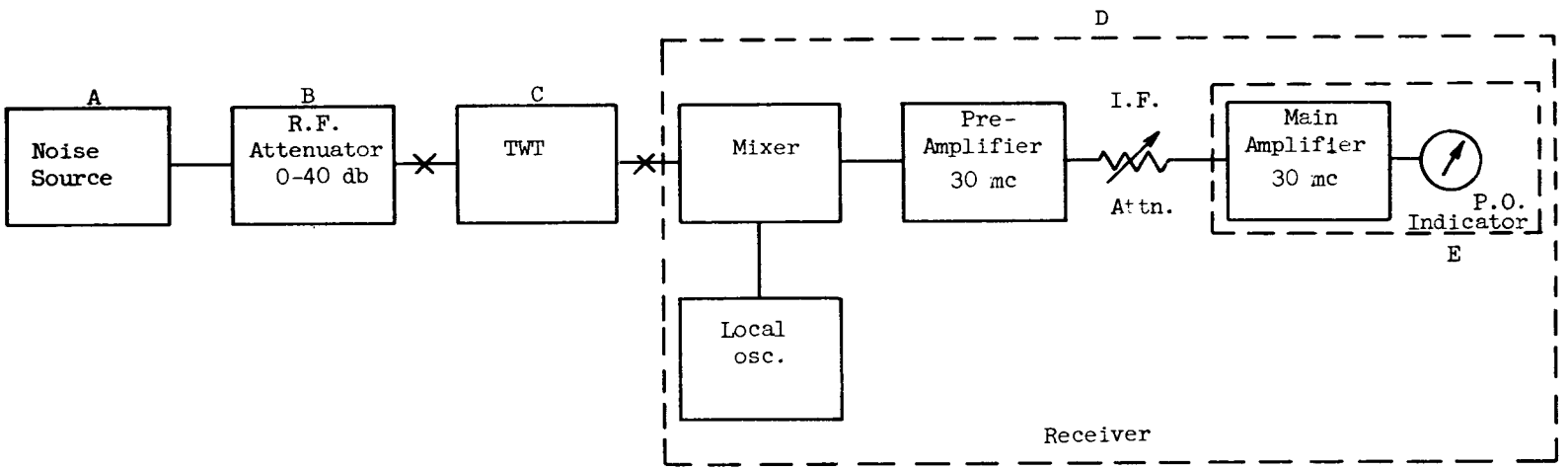

Item	Remarks
A	Waveguide Noise Source Waveline No. 2200-2 or Equivalent
B	RF Attenuators Standard Telephone and Cables, Ltd. Model 74600 or Equivalent
C	TWT under Test
D	Standard Microwave Test Receiver (I.F. $\cong$ 30 mc)
E	Hewlett-Packard Noise Meter, Model 340A, or Equivalent

Fig. 14 - Block diagram of the test setup used for measuring tube noise figures.

reading increases Y db. This ratio is determined by inserting if attenuation until the reading on the power meter is the same as has been determined with tube noise alone. The NF can be noted from convenient charts plotting the inverse function of Y versus NF. This NF includes receiver noise. In most cases, this is negligible if the receiver gain is high, but can, if required, be subtracted out.

Rapid and direct noise figure measurements can be made using an automatic NF measuring unit such as the Hewlett-Packard Model 340A. This unit is inserted in the receiver section marked (E) in Fig. 14.

In the measurement of tube noise figures of less than 5-db, extra care must be used in determining the amount of added noise (i. e., temperature effects become significant) and in calibrating all loss factors. Increased accuracy may be obtained by reducing the known noise input level with use of attenuator (A). For measurements of noise figure below 3-db, the known noise input level will be provided by means of an accurately calibrated termination, operated at two different temperatures, i. e., the hot-cold loss method.

The noise figure as measured above is not the "spot NF" but represents the average NF between two ranges of frequencies separated by twice the if frequency. The width of the range of frequencies is a function of the if bandwidth. This NF, measured without a filter to remove one of the sidebands, is either higher than the minimum "spot NF" or equal to it.

APPENDIX D

PHASE MEASUREMENTS

A brief literature survey was conducted in regard to phase measurement techniques and phase shift components. As a result of this survey, a phase shifter was constructed employing a trombone constant-impedance line stretcher and a precision mechanical drive. This phase shifter has a VSWR under 1.2 over the frequency range of 2500 to 3500 mc and over the range of phase shift adjustment available. A phase shift measurement system was constructed employing this phase shifter in a conventional phase-bridge.

Measured phase characteristics for the RCA type 6861 traveling-wave tube, which was used as the prototype for this developmental tube design, fall in the following ranges:

$$\frac{\Delta\phi}{\Delta E_h} = 8.22 \text{ to } 18.2 \text{ degrees/volt at } 2945 \text{ mc}$$

$$\frac{\Delta\phi}{\Delta Eg_2} = 6.0 \text{ to } 10.9 \text{ degrees/volt at } 2945 \text{ mc}$$

$$\frac{\Delta\phi}{\Delta Eg_1} = 5.0 \text{ to } 6.0 \text{ degrees/volt at } 2945 \text{ mc}$$

$$\frac{\Delta\phi}{\Delta Eg_1} = 10.0 \text{ to } 12.0 \text{ degrees/volt at } 3100 \text{ mc}$$

$$\frac{\Delta\phi}{\Delta Eg_1} = 9.0 \text{ to } 11.0 \text{ degrees/volt at } 3255 \text{ mc}$$

Phase measurements, made on a developmental tube and on one developmental sample tube based on this design, are plotted in Figs. 15 through 19. These measurements indicate that the phase characteristics of the new developmental tube design remains essentially similar to that of the original prototype 6861 design even though operating conditions are drastically different in each design.

Attenpts to measure $\frac{\Delta\phi}{f}$ for the developmental tube design were suspended since doubtful results were expected if hurried measurements were made on this complicated test set-up.

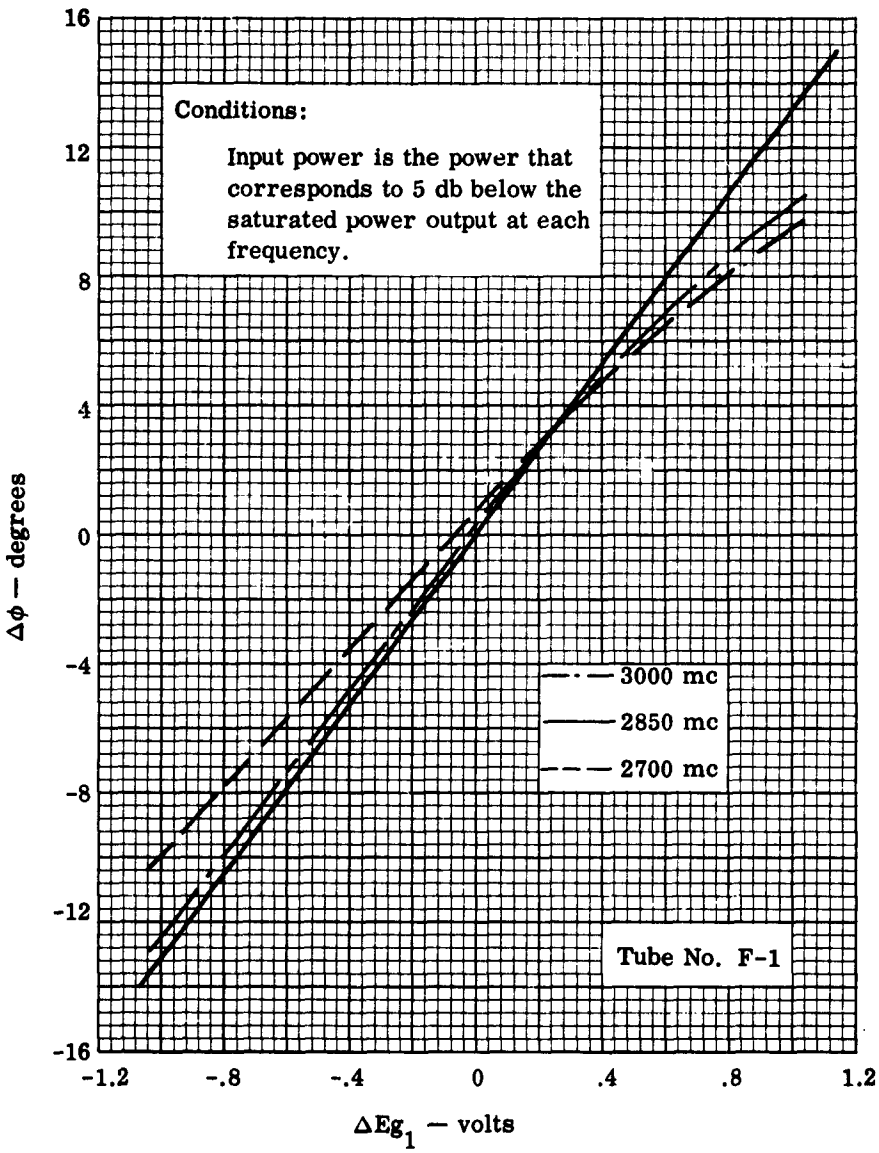

Fig. 15 — Changes in the phase of the signal ($\Delta\phi$) as a function of the potential variation on grid No. 1 (ΔEg_1) for a developmental tube

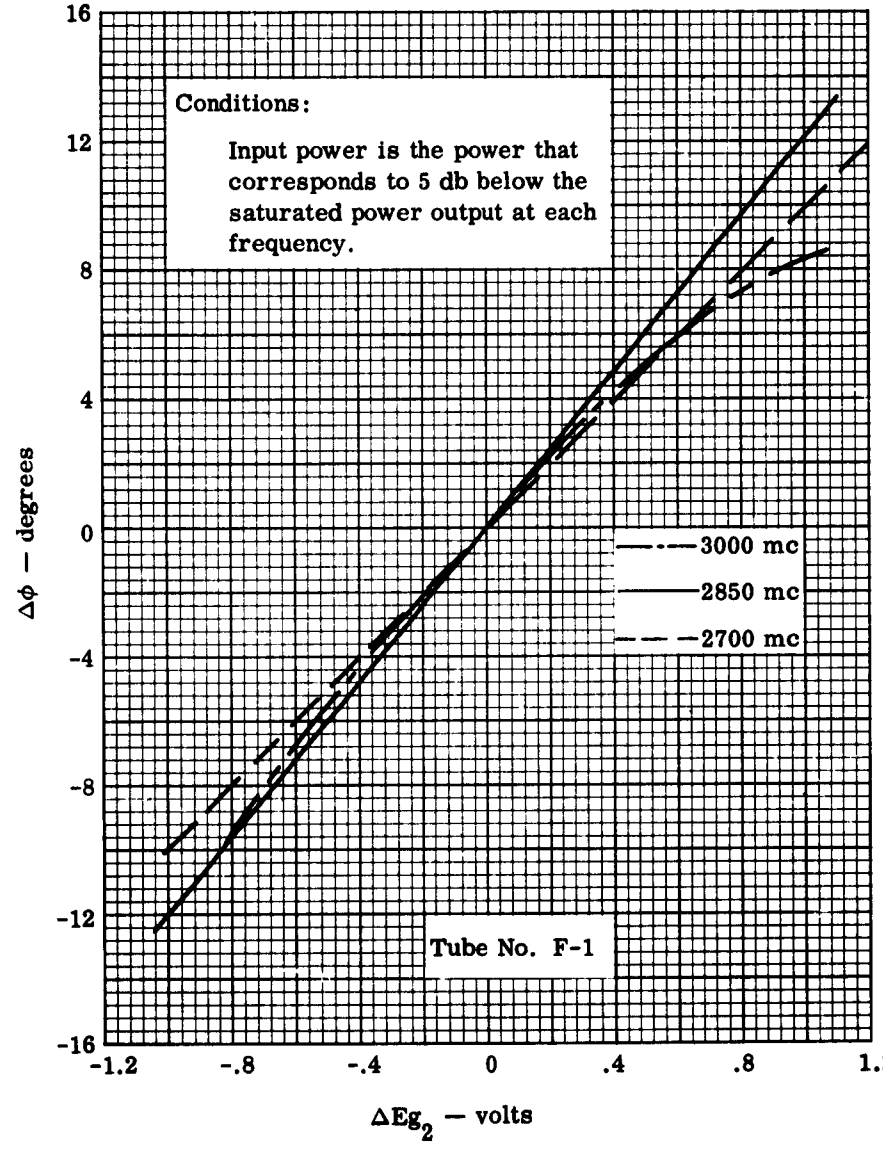

Fig. 16 — Changes in the phase of the signal ($\Delta\phi$) as a function of the potential variations on grid No. 2 (ΔEg_2) for a developmental tube

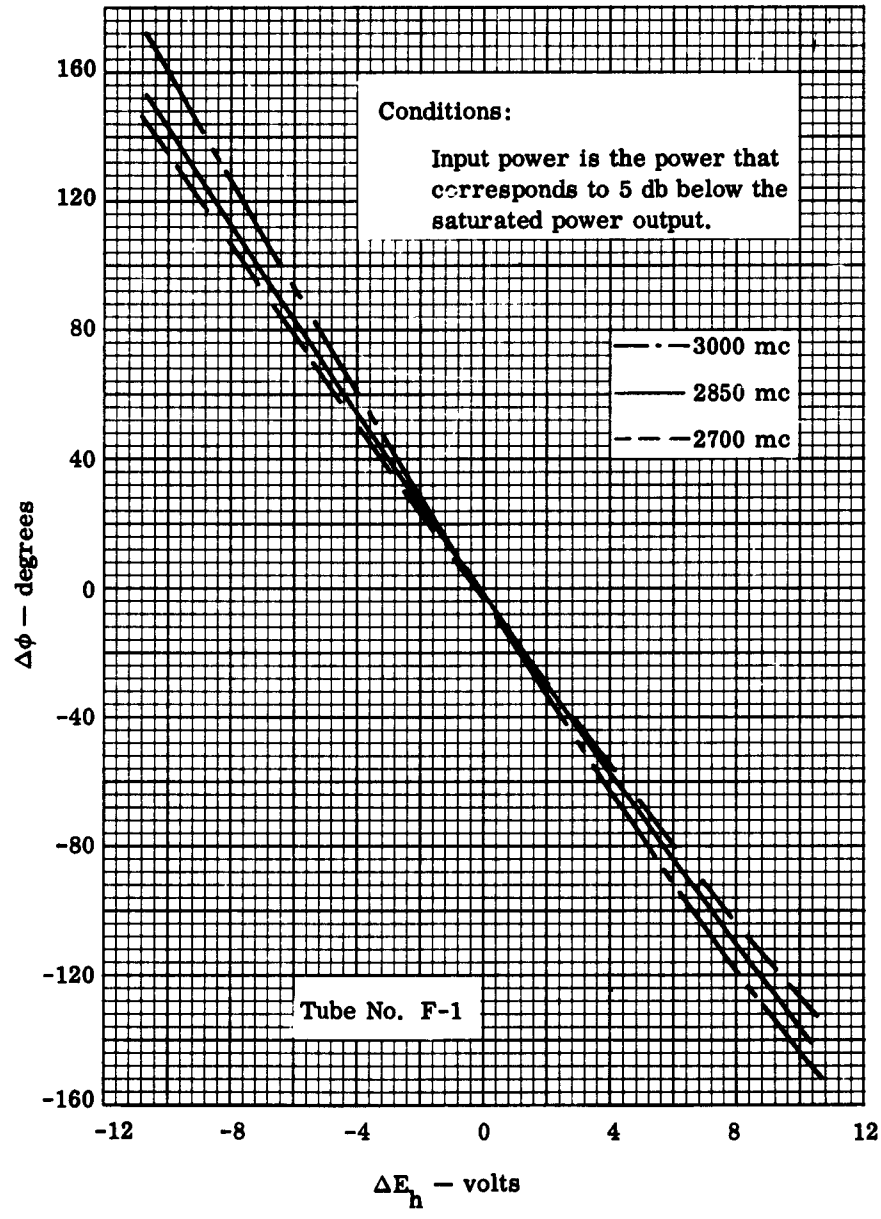

Fig. 17 — Changes in the phase of the signal ($\Delta\phi$) as a function of helix voltage variations (ΔE_h) for a developmental tube

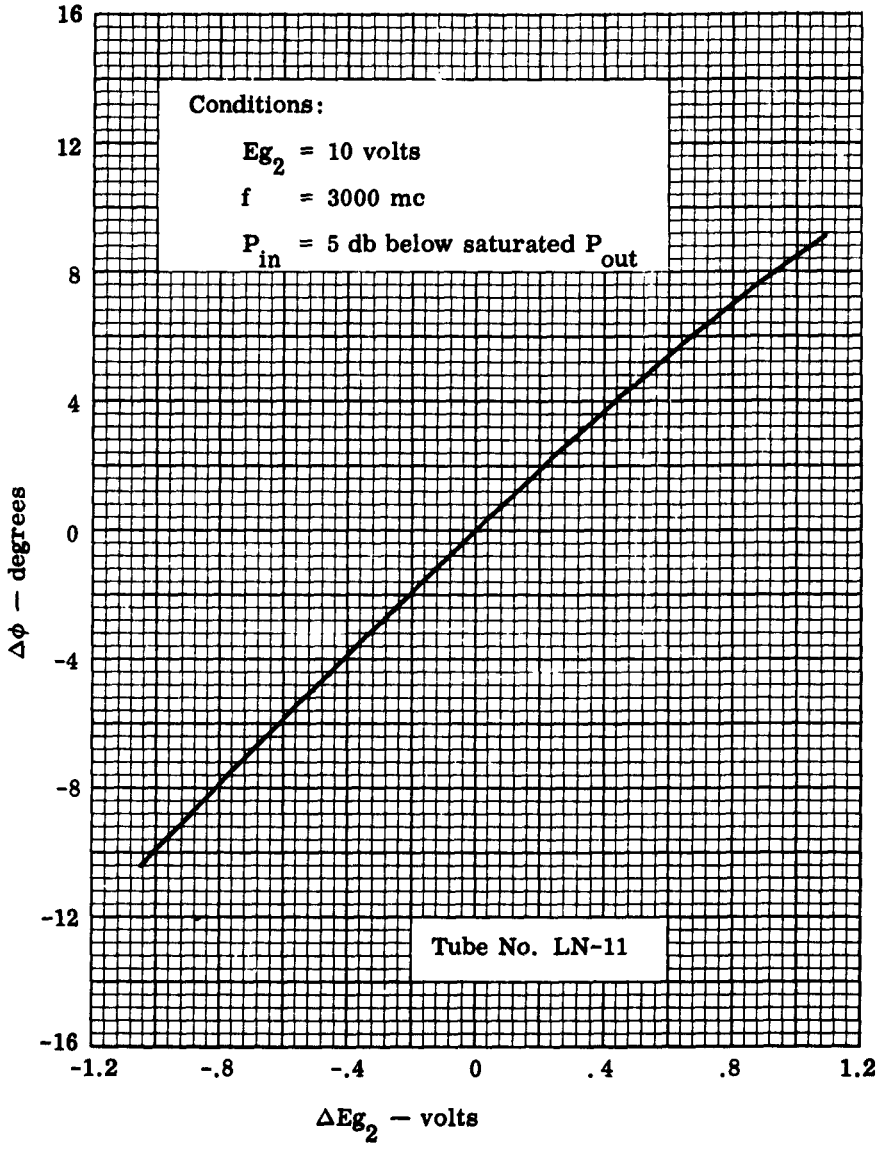

Fig. 18 — Changes in the phase of the signal ($\Delta\phi$) as a function of the potential variations on grid No. 2 (ΔEg_2) for an experimental sample tube

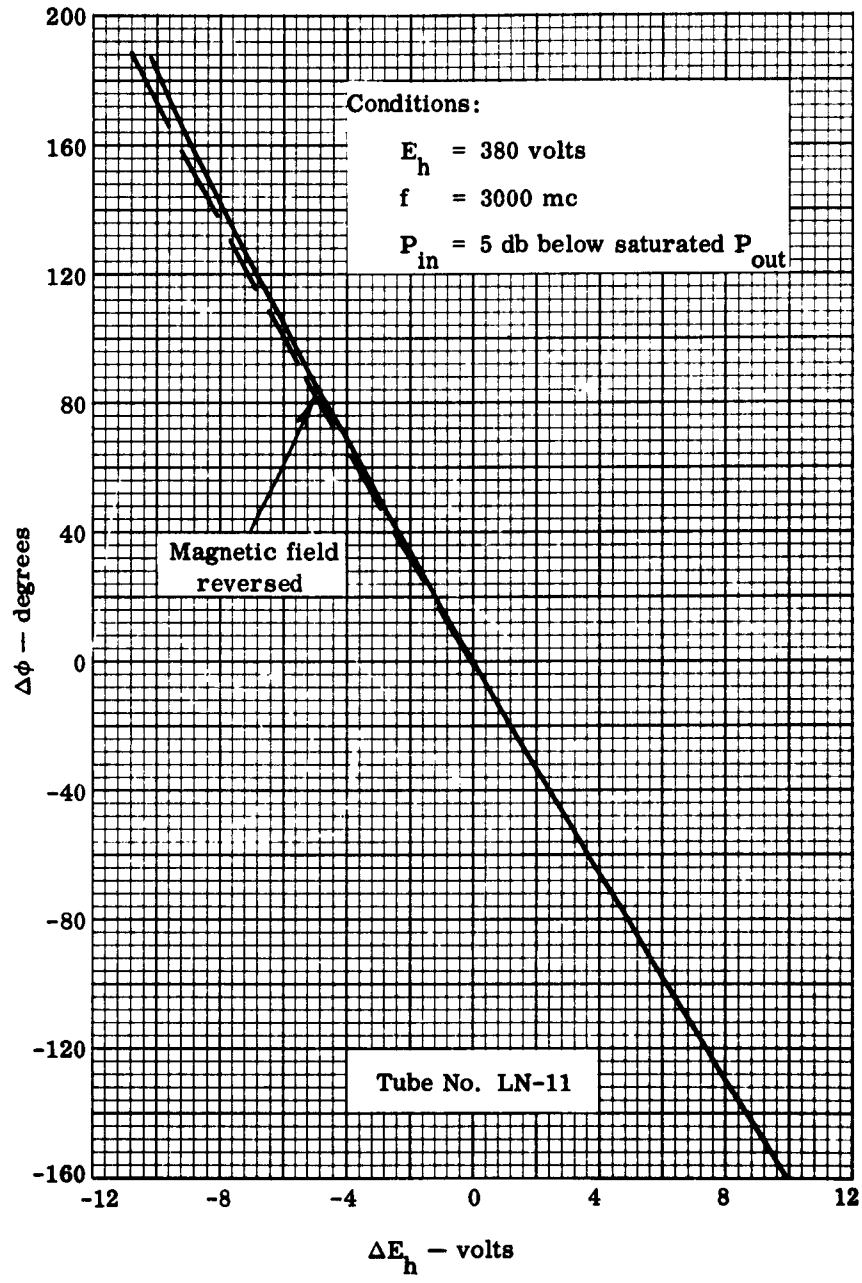

Fig. 19 — Changes in the phase of the signal ($\Delta\phi$) as a function of helix voltage variations (ΔE_h) for an experimental sample tube